Stress Transfer Between Multi-Seam Longwall Mines

by

Rajive Ganguli

Thesis submitted to the Faculty of the

Virginia Polytechnic Institute and State University

in partial fulfillment of the requirements for the degree of

MASTER OF SCIENCE

in

Mining and Minerals Engineering

APPROVED

Dr. Christopher Hayccks
(Chairman)

Dr. Michael Karmis
(Head of the Department)

Dr. John Wilson
(University of Missouri, Rolla)

May 10, 1995

Blacksburg, Virginia

Keywords: Multi-seam, Layering, Stress Transfer, Photoelasticity, Longwall

STRESS TRANSFER BETWEEN MULTI-SEAM LONGWALL MINES

by

Rajive Ganguli

Dr. Christopher Haycocks, Chairman

Department of Mining and Minerals Engineering

ABSTRACT

The future of most underground coal mining in the USA will entail the extraction of coal under multi-seam mining conditions. Mine design in such an environment will require the accurate prediction of stress transfer between adjacent seams. The available knowledge on criteria controlling stress transfer has been exhaustively reviewed and critical factors affecting multi-seam mining investigated. Young's Moduli of rock layers, thickness of rock layers, number of these layers and the coefficient of friction between these layers were identified as important parameters which affect stress transfer from mining of one seam to another. These parameters were studied using photoelastic methods and results analyzed both qualitatively and quantitatively. Finite element studies were also performed using UTAH2PC. Data obtained from field studies was used to correlate laboratory findings with prototype observations. Excellent correlation was obtained between laboratory and field data. Validity of the research is demonstrated using case studies.

AKNOWLEDGEMENTS

The author is deeply indebted to Dr. Christopher Haycocks his major advisor, for his constant guidance and motivation. The valuable comments of Dr. Michael Karmis, Head of the Department and Commmittee member, and Dr. John Wilson, University of Missouri-Rolla, are gratefully acknowledged.

The author would like to thank his parents for their constant moral support.

TABLE OF CONTENTS

List of Figures

Figure		Page No.

Figure		Page No.

List of Tables

Chapter 1

INTRODUCTION

1.1 Statement of the Problem

The use of the longwall method of mining continues to increase across the United States, particularly in multi-seam environments. Total longwall production in the US is expected to increase from 151 million tons per year (tpy) in 1995 to 172 million tpy in the year 2000 (Weisdack, 1995). In the Appalachian coal fields, design problems have a special urgency since the majority of the coal mines occur in a multi-seam environment as shown in Figure 1.1 (Hudock, 1983; Wu, 1987). According to one estimate, 156 of the 229 billion tons of bituminous coal that can be mined in the US may be subject to seam interaction (Engineers International, 1981). Virgin unmined areas are becoming a rarity, and it is now usual to mine in the vicinity of other mine workings (Haycocks, 1991; Akram et al., 1993).

Siting longwalls in either upper and/or lower seams is complicated due to the active and passive stress fields that develop both during and after mining in either seam. The high capital costs of longwall equipment and the limited flexibility in the system once the gate roads are in place, make correct initial design essential.

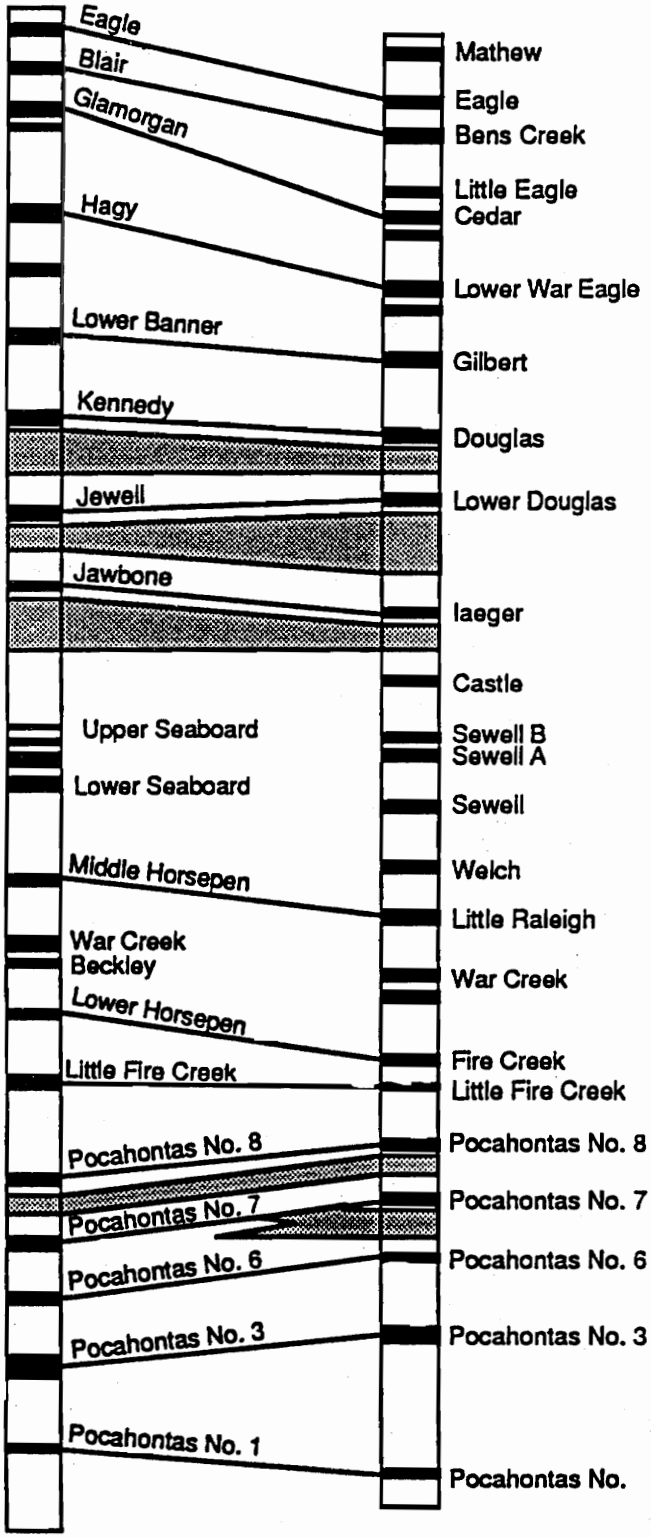

Figure 1.1 Typical multiple seams in a mine property (After Zhou, 1989)

Implementation of this design requires accurate specification of the loads that will be carried by the gate road entries and pillars. This can be done for single seam mining, but new techniques must be developed to predict the effects of interaction between longwall installations operating in a multi-seam environment.

Previous research has concentrated on methods for minimizing the effects of interaction by considering only static loading conditions and utilizing yield pillar concepts. The unique aspects of dynamic longwall forces, including the high stress transfer distances of over 220 m (760 ft.), make them unpredictable when using conventional numerical modeling methods and thus specialized analytical techniques are required.

1.2 Objectives and Methodology of Research

There are many factors, both mining and geological, which are known to control stress transfer created by mining between seams (Zhou, 1988; Haycocks and Zhou, 1990; Haycocks, 1991). These can be considered as either *controllable* or *uncontrollable* parameters. Examples of these are :

<u>Uncontrollable</u>

-- geology and structure

-- depth to upper seam

-- innnerburden thickness

-- stress field including depth

-- water

Controllable

-- timing between mining

-- mining system

-- spatial layout factors

During mining some of the operational parameters may be altered to accommodate or even offset the naturally occurring adverse factors (Peng and Chandra, 1980). Hence, it is important that the effects of natural factors be studied, defined and quantified. One such natural factor, layering of the strata, is known to affect stress transfer (Gaziev and Erilikhman, 1971; Chekan et al., 1994). The objective of this research was to study the effects of layering on stress transfer from upper to lower seams. Most aspects of layering were studied in this research, including thickness of the layers, number of layers, strength of layers and friction between layers, in order to predict their effects on stress transfer. Since applying theoretical and numerical concepts to rock is difficult because of discontinuities, photoelastic methods were selected for the study. Where relevant, finite element analyses were carried out to further expand the photoelastic results.

Chapter 2

LITERATURE REVIEW

Four mechanisms have been identified that can control interaction between the working of adjacent seams :

-- stress transfer above and below remnant pillars

-- arching of strata above and below seams

-- trough subsidence

-- block shearing

Of these mechanisms the first two involve load transfer. Research has demonstrated that the following factors play a major role in determining the magnitude and extent of this stress transfer (Holland, 1951; Zhou, 1988; Haycocks, 1991):

1) mining method practiced in each seam
2) extraction ratio
3) innerburden thickness
4) mining height in both seams (workings)
5) nature of innerburden
    - -- number of layers
    - -- thickness of various layers
    - -- moduli of the layers

-- interlayer friction.

Two basic concepts, pressure bulb and pressure arch, have been developed to explain and quantify stress transfer between seams. The pressure bulb theory can be applied to explain stress transfer above and below pillars and/or other remnant structures. Pressure arch concepts are used to evaluate stress transfer around and between mine openings.

2.1 Pressure Bulb Concept

Stress transfer in a homogeneous elastic medium was studied by Boussinesq (1885). He theorized that the vertical load effectively dissipated at a depth of three times the loading width, as shown in Figure 2.1. Huang (1968) thought Boussinesq's theory was conservative for soils and unusable for rocks. Giroud (1970) contended that homogeneity of strata has little effect on stress transfer. Gerrard (1967) found that stiff layers limited the distance of stress transfer. Haycocks and Karmis (1983) reached a similar conclusion, based on the analysis of field data from room and pillar mines as shown in Figure 2.2, and their data was summarized with the equation :

$$D = 110 - 0.65\,S \qquad (2.1)$$

where,

D = the minimum stable innerburden distance in feet

S = the percent hard rock in the innerburden.

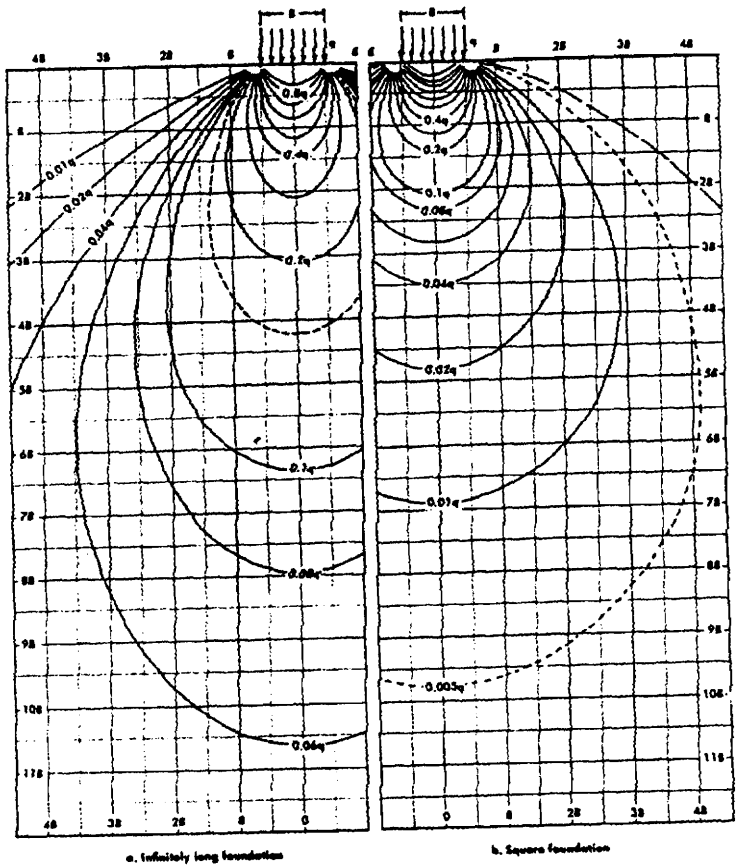

Figure 2.1. Boussinesq's Analysis - vertical stress contours in isotropic media proportional to uniform foundation pressure (After Sowers, 1979)

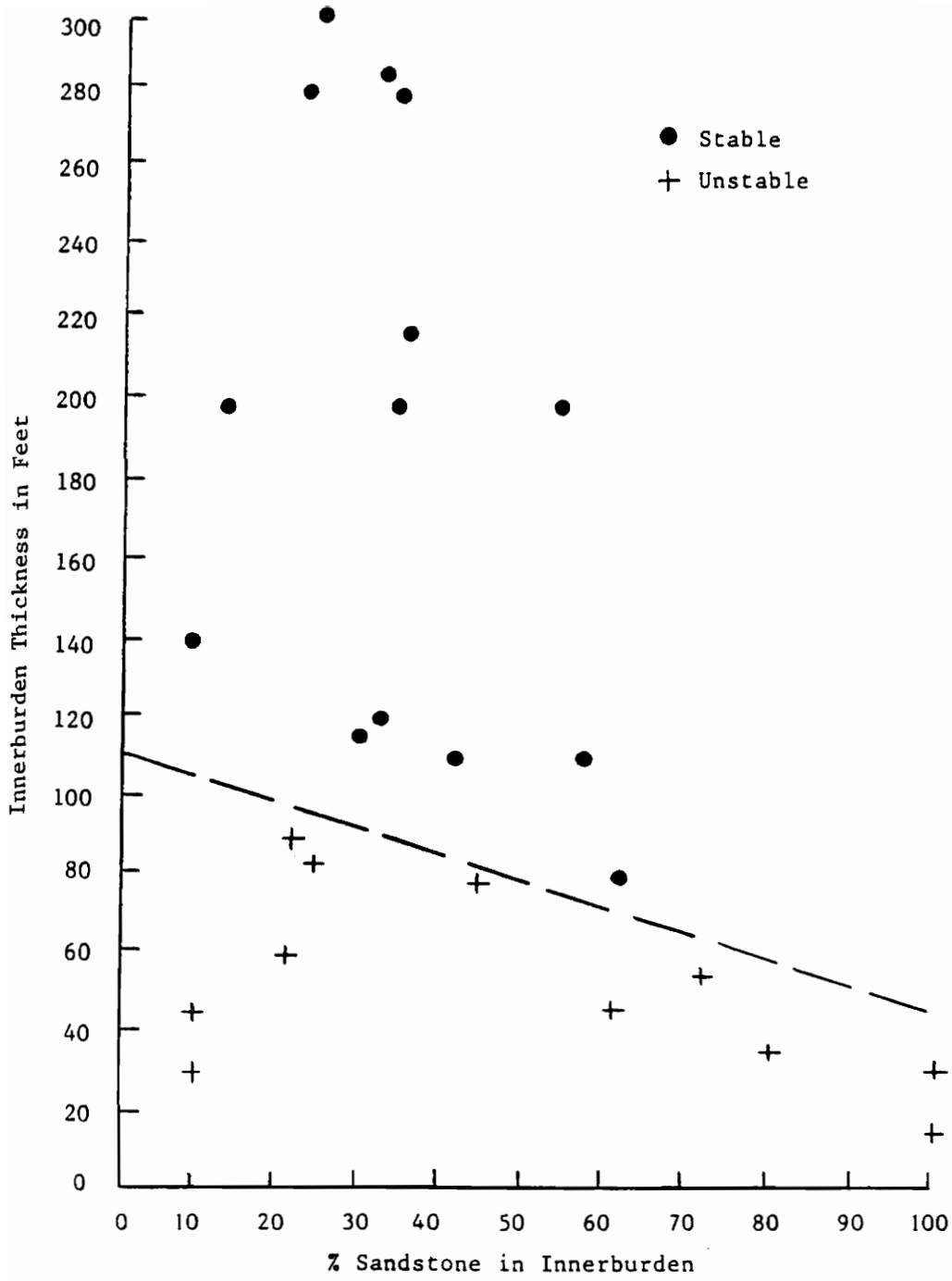

Figure 2.2 Effect of sandstone in innerburden on stability (After Haycocks and Karmis, 1981)

Between room and pillar mines, the maximum distance of stress transfer resulting in damage to workings in the lower seam is 110 feet, with no hardrock in the innerburden.

Gravity loaded, low modulus photoelastic models were used to demonstrate the effect of layering on stress transfer, with results similar to the effects of rigid layers in the innerburden (Ehgartner, 1982). This work showed a vertical distortion of the pressure bulb with an increase in layering. The minimum innerburden thickness required for stability in a non-layered material was only 15.6 m (52 feet), while 10 layers of strata require at least 36 m (120 feet). Ehgartner (1982) summarized his findings with the equation :

$$D = 6.8\,N + 55 \qquad (2.2)$$

where,

D = minimum stable parting thickness in feet

N = the number of beds in the interval

A high modulus of elasticity in some of the layers concentration of the stresses (Ehgartner, 1982; Su et al., 1986). Figure 2.3 shows the lateral extent of the stress for different layers. From this figure, it is evident that for low modulus layers, the horizontal spread of the pressure bulb is increased.

Ehgartner (1982) noted that stress transfer depended in part, on the distribution of loading in the pillar. He based his study on four stress forms that

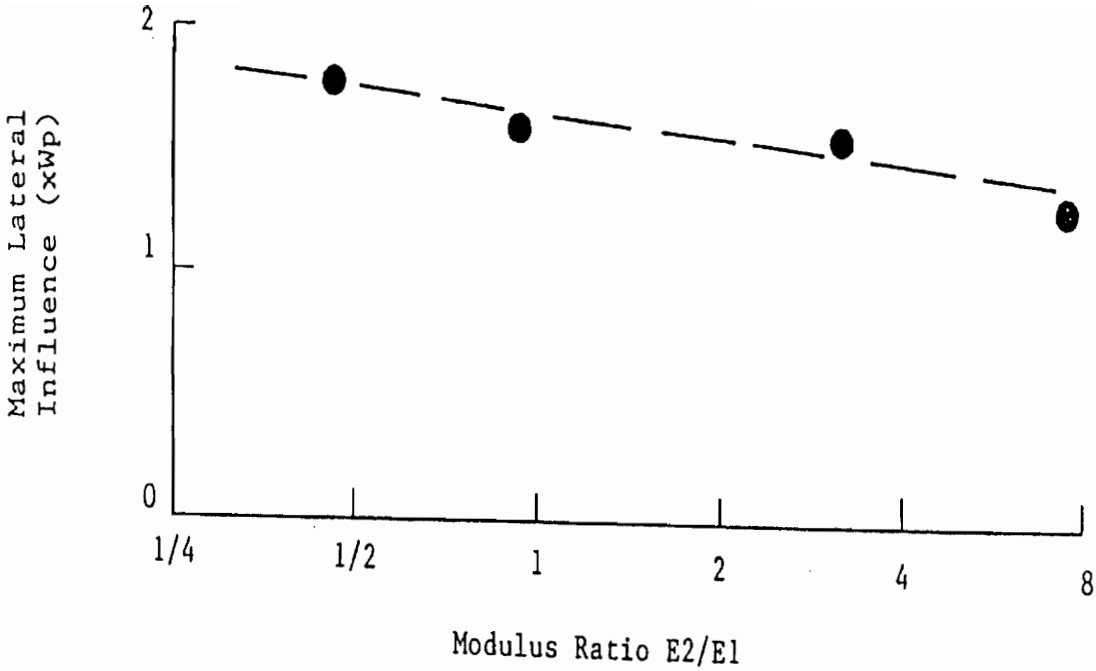

Figure 2.3 Modulus of Elasticity of layers vs. horizontal extent of vertical stress (After Ehgartner, 1982)

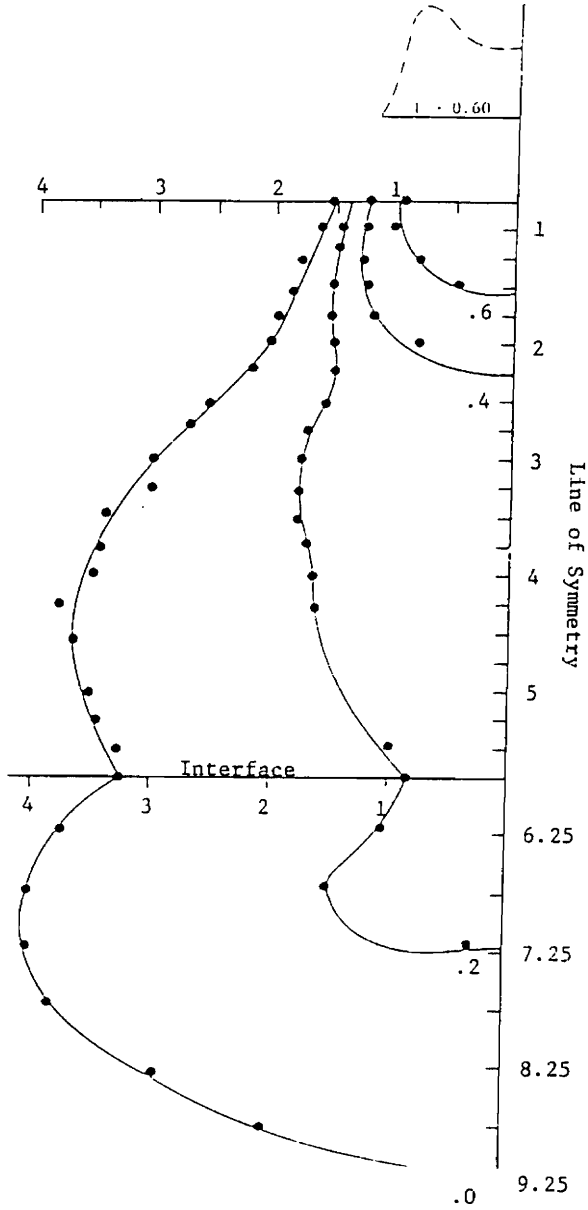

Figure 2.4 Pressure bulb distortion under a 1-.60 stress form (Ehgartner, 1982)

had different ratios of peak and trough loading. Figure 2.4 shows the pressure bulb for a particular stress form. By doing this he could simulate different pillar loading conditions such as for small and large pillars. For example, small pillars were generally uniformly loaded throughout their cross-section, which means that the ratio of the peak and trough loads was 1. For a large pillar, which has peak loads at the edges and low loads (trough) at the center, the ratio of peak load to trough load could be as high as 4. Ehgartner concluded that stress transfer was increased for uniform loads in comparison to trough loading.

There is, however, no report in the literature on the effects of thickness of layers on the width of the pressure bulb. Some mention was made of the effect of slippage between layers and layer inclination (Gaziev et al., 1971; Peng, 1986). Figure 2.5 shows some effects of layering on stress transfer, and the distortion of the pressure bulbs can be easily noted. Slippage between layers is expected to increase the distance of stress transfer, while layer inclination distorts stress contours.

2.2 Pressure Arch Theory

The pressure arch theory dictates that a high pressure zone would form in an elliptical shape above an opening, while the area under the arch would be de-stressed. Fayol (1885) was the first to propound this theory. He proposed a "dome" which limited the movement of strata. If the excavation was large, then

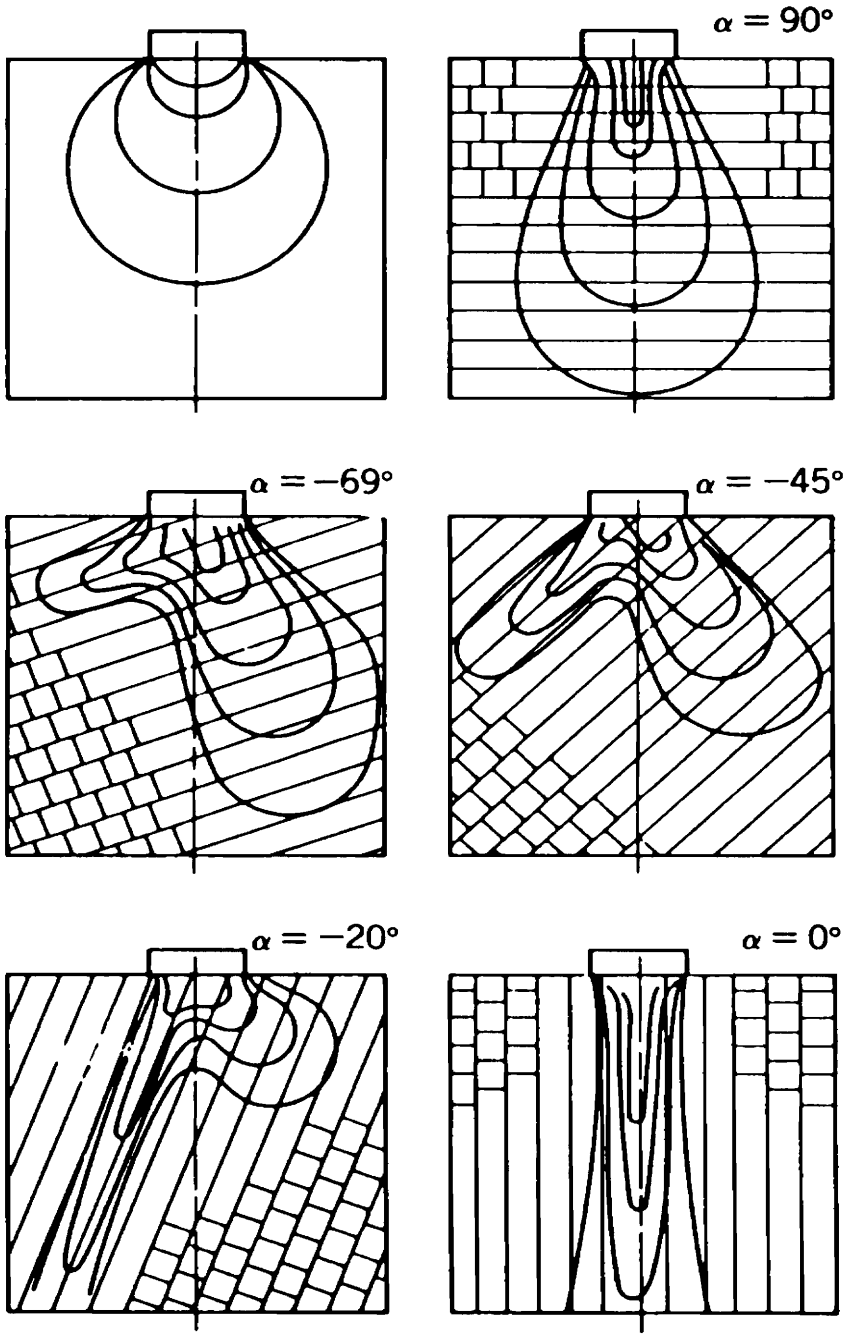

Figure 2.5 Effect of layering on stress (Gaziev et al., 1971)

the movement of strata was limited to a height less than 200 times the extraction height. For an excavation of limited area, the arch theory suggests that the height of the dome is two to four times the width of extraction. For seams of height 2 m or less, the height of the dome is twice the width of extraction and increases with increased extraction height. He believed roofs consisted of independent beams which failed due to shear. Many other researchers supported the shear failure theory (Barko, 1982; Haycocks, 1991). Fayol's dome is shown in Figure 2.6.

The formation and dimensions of the arch are dependent on various factors such as excavation dimensions, strata properties, stress values and time. Regarding the shape of the arch, Randolph (1915) was of the opinion that the position and type of forces acting on the arch would have an effect on the shape of the arch. For hydrostatic pressure conditions, the shape would be semi-circular, while for high stresses at the center, the shape would be parabolic. Layers of different materials will cause distortion in shape to maintain equilibrium.

One of the major advances in the pressure arch theory came from Dinsdale (1937). Figure 2.7 explains the various terms required to understand his theory. *Superincumbent pressure* or *undisturbed pressure* is the pressure of the virgin strata. An opening leads to the formation of a pressure ring around itself. A part of this superincumbent pressure (the weight of the ground above) is deflected to the sides of the opening or abutment. This pressure is called

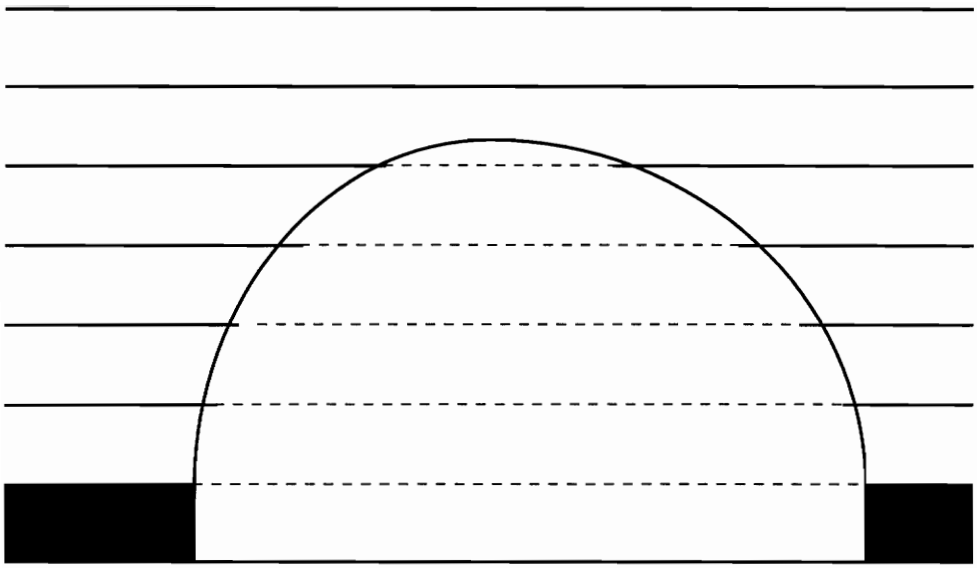

Figure 2.6 Fayol's Dome (After Fayol, 1885)

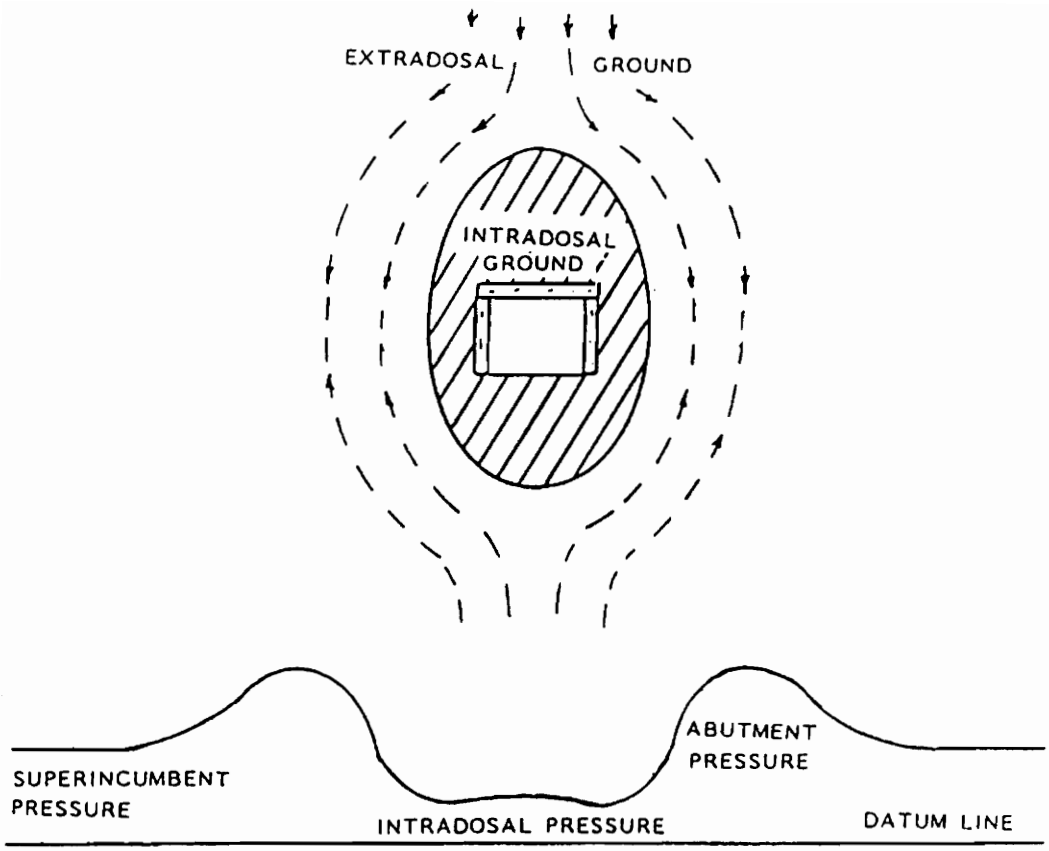

Figure 2.7 Terminology of Dinsdale's pressure arch theory
(After Dinsdale, 1937)

abutment pressure. Inside the ring is a de-stressed region known as the *intradosal* ground (tension zone). On the periphery of this intradosal ground there is a zone of compressed ground called *extradosal* ground (compression zone). Other researchers also found the same pattern of tension and compression zone (Chekan et al., 1986). The height of the intradosal ground depends on the strata pressure and the type of material forming the intradosal ground. The height and span of the arch increases with the increase in excavation width until its failure, when subsidence occurs.

Denkhaus (1964) proposed a few theories to explain the pressure arch concept in different strata conditions. Rigid dome theory, elastic dome theory, and beam and plate theory were proposed by him to explain the pressure arch phenomenon. While the rigid dome and elastic dome theories deal with the strata as homogeneous and isotropic, the beam and plate theory considers the strata as stratified. Beams are used to explain the theory in two dimensions while the plate is for three dimensions.

2.2.1 Pressure Arch Shape and Size

Three shapes of pressure arch are possible (Hudock, 1983) :

1) elliptical
2) parabolic and
3) an alteration of the above.

Mohr (1956) proposed a theory which holds good for massive and intact rock. He proposed the relationship :

$$B / L = ZZ / XX = (1-PR) / PR \quad -- \quad -- \quad -- \quad -- (2.3)$$

where,

B = the height of the dome from the central axis

L = the semi-width of the dome

ZZ = the vertical stress

XX = the horizontal stress

PR = Poisson's ratio

For hydrostatic conditions the arch becomes semicircular in the arch theory. This is similar to the prediction of Randolph's theory (1915). Randolph's theory also predicts that the height of the dome depends on the nature of the strata, with stronger strata generating higher arches. National Coal Board researchers (1954) theorized that the pressure bulb extended as far below the seam as it does above and when there is superposition of the arch abutments, the stresses are additive. Figure 2.8 shows superposition of arch stresses. According to the findings of the National Coal Board the strata is under great pressure for 20-30 yards beyond the intradosal zone after which the stress returns to normal. The height of the pressure was theorized to be about twice the width of the pressure arch. For depths between 400 and 2,000 feet they proposed a relationship:

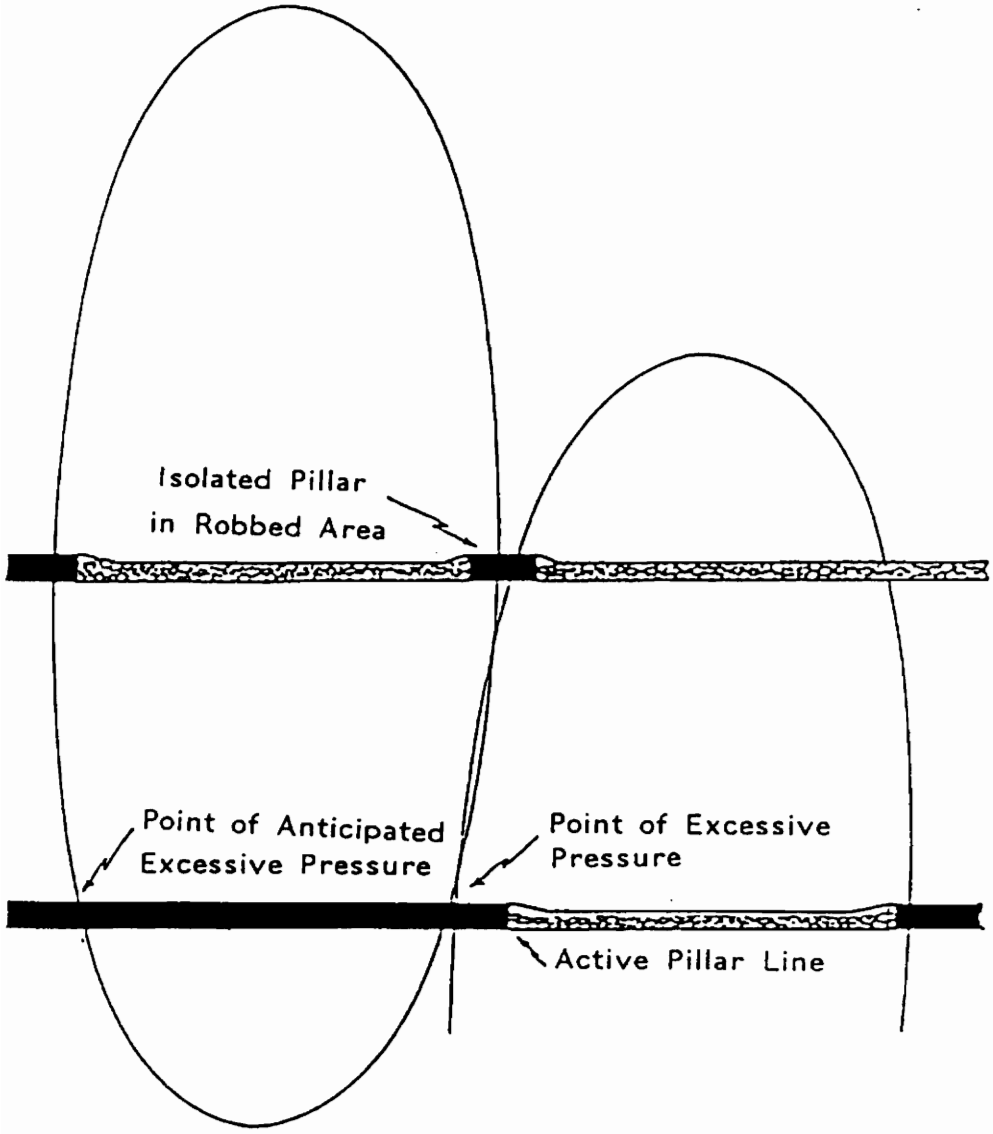

Figure 2.8 Superposition of arches (After Stemple, 1956)

$$W = D / 20 + 20 \quad -- \quad -- \quad -- \quad -- (2.4)$$

where

W = width of the maximum pressure arch in yards, and

D = depth of the seam below surface in feet.

2.3 Strata Mechanics in Longwall Operations

Longwall operations accounted for approximately 23% of US underground coal production in 1984 (Peng, 1986). Improved technology and safety are rapidly increasing the share of longwall mining in coal production. Technology to improve the design of longwall installations is therefore becoming increasingly important. Figure 2.9 shows a typical longwall layout.

When an opening is created, the in-situ stress equilibrium is destroyed and the stress is redistributed to create a new state of equilibrium. A pressure arch is formed, creating a de-stressed zone above the roof of the opening and transferring the load onto the neighboring coal surrounding the mined out area. Thus, near the edges of the panel and pillars the average stress is greater than the overburden pressure. These regions are known as *abutments* and the pressure there is known as the *abutment pressure*. Figure 2.10 shows the abutment pressure in a typical longwall operation. The stresses created during mining are superimposed with those created during entry development. *Front abutment pressure* is found in front of the face while *side abutment pressures* occurs along both sides of the panel in the gob area. The front and side

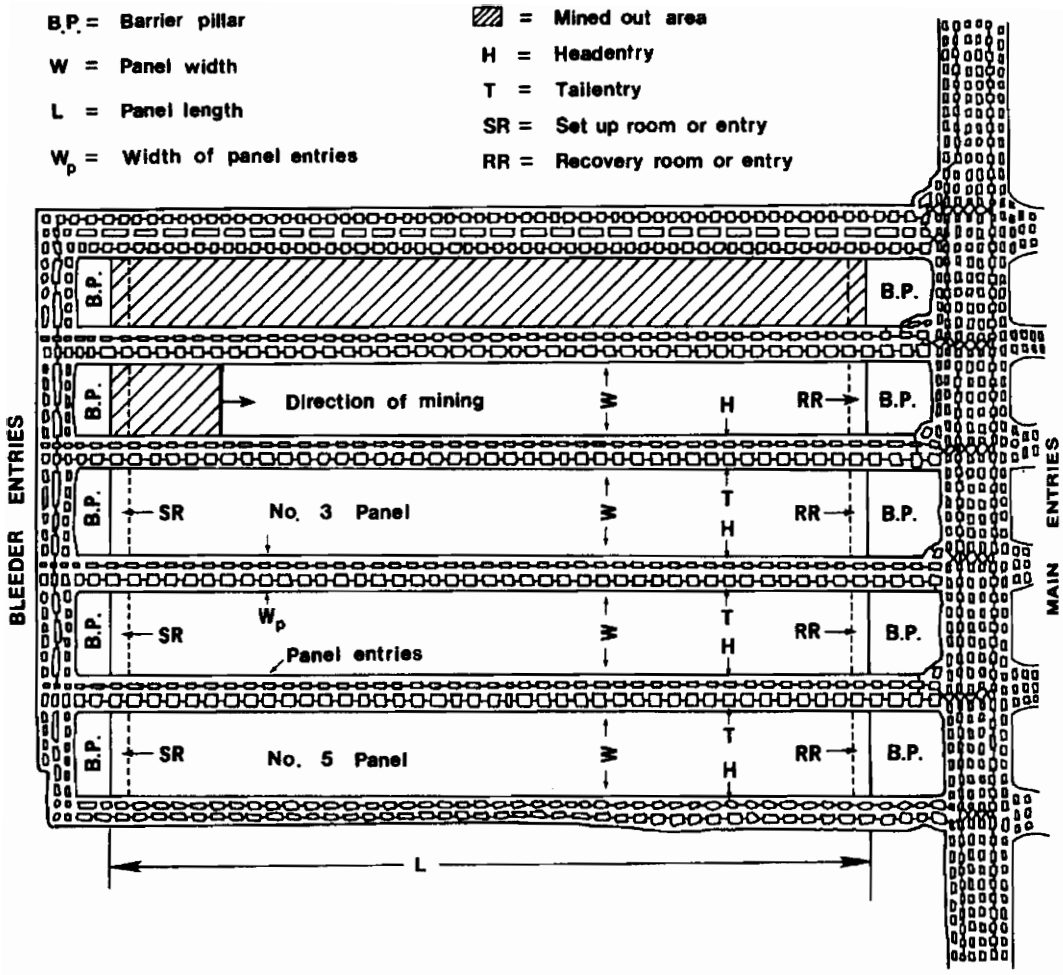

Figure 2.9 Typical longwall layout (Peng and Chiang, 1984)

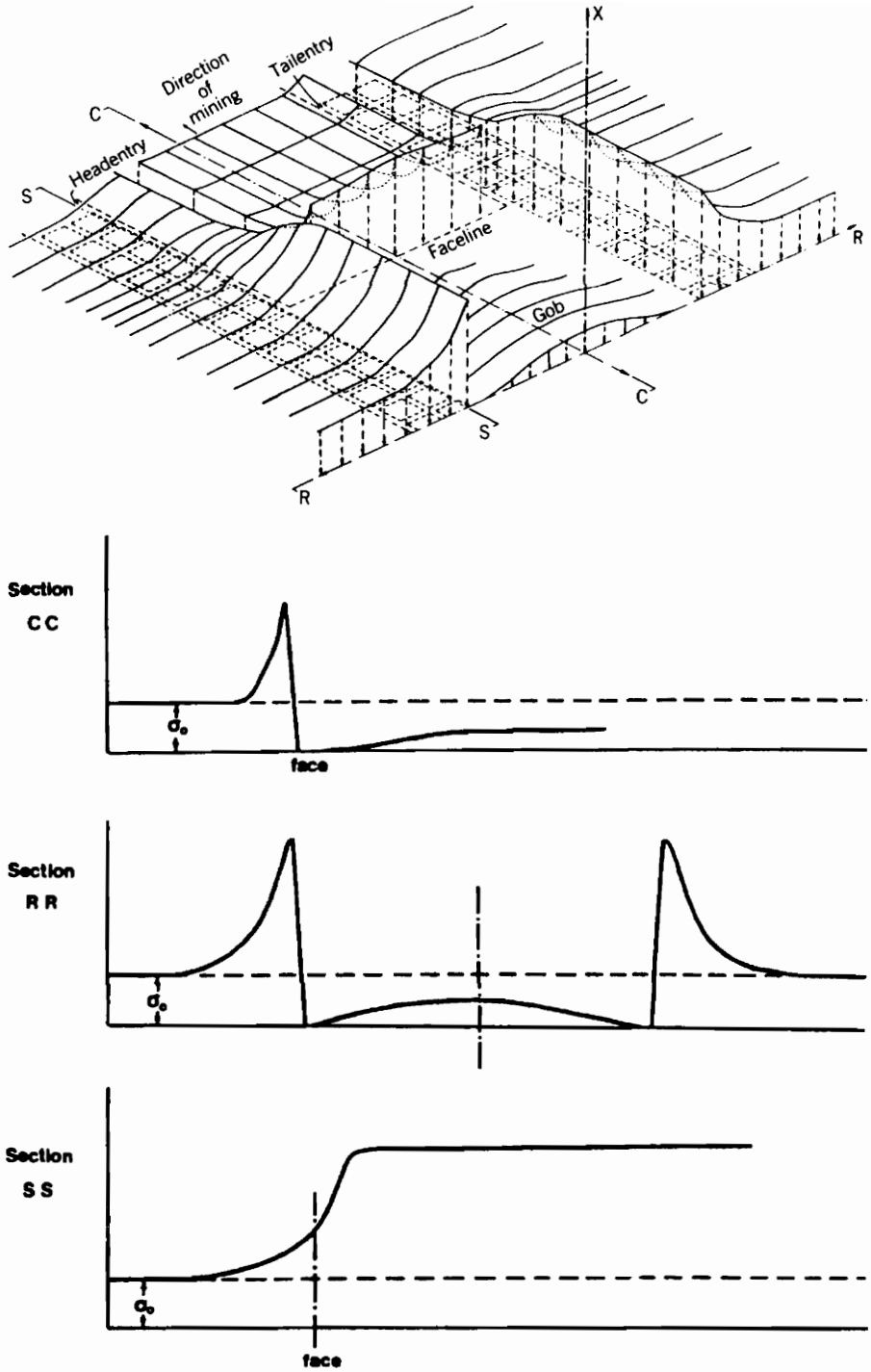

Figure 2.10 Stresses in a typical longwall operation (Peng and Chiang, 1984)

abutment pressures superimpose at the corner of the panel. The characteristics of the roof strata control the location of the peak front abutment for both the center and the corner of the panel (Peng, 1986).

Front Abutment Pressure : The front abutment pressure can be detected at a distance of one times the overburden depth from the face. The magnitude increases slowly as it nears the face and at about 100 ft. from the face it starts to increase rapidly. It reaches its maximum value at a distance of 3-20 ft. from the face and drops to zero at the face itself (section CC in Figure 2.10). The maximum front abutment pressure is not uniformly distributed. In general, the magnitude of the maximum front abutment pressure ranges from **0.2** to **6.4**σ_0 (where σ_0 is the average in-situ overburden pressure) depending on the geological conditions, face location with respect to the periodic roof weighting and the setup entry, and the adjacent mined-out areas (Peng, 1986).

Side Abutment Pressure :

At about the same time the front abutment is felt, the side abutment is felt at the ribs of the head-entry and tail-entry. The side abutment pressure increases as the face advances while extending away from the face (section SS in Figure 2.10). While at the ribs of the head and tail entries the side abutment pressure is the largest, it drops exponentially away from the panel. At the first

row of chain pillars the side abutment pressure ranges from **0.4** to **3.5**σ_0 depending on the location inside the panel. The side abutment pressure continues to extend outward from the active faceline up to a certain distance. The width of the side abutment, W_s, is given in feet by the equation (Peng, 1986):

$$W_s = 9.3\sqrt{h} \qquad \text{-- -- -- -- -- (2.5)}$$

where h is the overburden depth in feet.

Gob Pressure : The weight of the caved roof material forms the initial gob pressure until it starts taking some of the load from the main roof (Peng, 1986). The maximum gob pressure occurs when the gob takes the full weight of the overburden. The unbroken strata remains bridged by the side abutments if the panel is narrow. In such situations the gob pressure is almost equal to the weight of the caving height.

2.4 Stress Prediction Between Longwall Faces

Recommendations for longwall layouts in a multi-seam environment were made that considered changes in pillar dimensions (Scurfield, 1970). Utilizing the de-stressed gob zone to protect lower seam workings was another alternative in design (Whittaker and Pye, 1975). These recommendations were based on field experience and lacked quantification for precise design.

Predicting the magnitude and distribution of stress transfer between longwall faces during lower seam multi-seam mining was first attempted using laminated, gravity loaded, photoelastic models (Forrest et al., 1988). This research clearly identified relevant mechanisms and stress distributions but was unable to quantify the results, which is required for actual design.

The finite element method has been used for several years to model mining situations (Iannachione, 1990; Akram, 1993). This method uses variational methods and interpolation theory for solving differential equations of initial and boundary value problems (Desai and Abel, 1972).

There are limitations to using this method, especially when model layering is considered to be important, although some limited success in modeling of inter-bed slippage has been reported (Iannachione, 1990). The code UTAH2PC, which was used for this research, had limited capability as far as modeling of layering was concerned (Pariseau et al., 1992). The method assumes perfect bonding between layers, and thus, the effect of slip between layers is not analyzed (Kripakov et al.,1994). Hence, the severity of stress transfer as seen in photoelastic models is not seen in finite element models.

The numerical modeling technique MULSIM/NL was used to illustrate and produce a stress transfer factor for undermining (Beckett and Madrid, 1988; Chekan and Listak, 1992;Chekan and Listak, 1993). Because of model limitations, however, predicted stress transfers seem to be far below those experienced in many field situations. The program utilized the results of the

ALPS program (Analysis of Longwall Pillar Stability) developed for single-seam longwall pillar design (Mark and Bieniawski, 1986; Mark, 1990; Mark, 1991). This design tool was also developed using numerical modeling and calibrated using large quantities of empirical data. Results from this work predicted a maximum stress of only 1.6 times the single-seam stress when a longwall face crosses under a gob-coal boundary, and only 1.8 times the single-seam stress when it is below an isolated gate road. The innerburden was assumed to be 50 feet and the depth to the upper seam 800 feet. The coal bed was assumed to be 6 feet thick.

While the importance of the innerburden conditions in stress transfer was acknowledged, no special mention was made of the effect of layering in the innerburden. Thus, the method totally under estimated the distance of stress transfers observed in the field. Under longwall mining conditions stress transfer between seams of more than 700 feet has been reported (Scurfield., 1970). These figures are orders of magnitudes higher than for room and pillar mining, probably reflecting the higher stresses developed during the active phase of longwalling. Figure 2.11 shows the effect of depth on stress transfer for various types of mining.

An initial modification of the stress transfer factor to more accurately describe mining conditions was attempted by incorporating a pressure bulb distortion factor based on field and model studies (Akram et al., 1993).

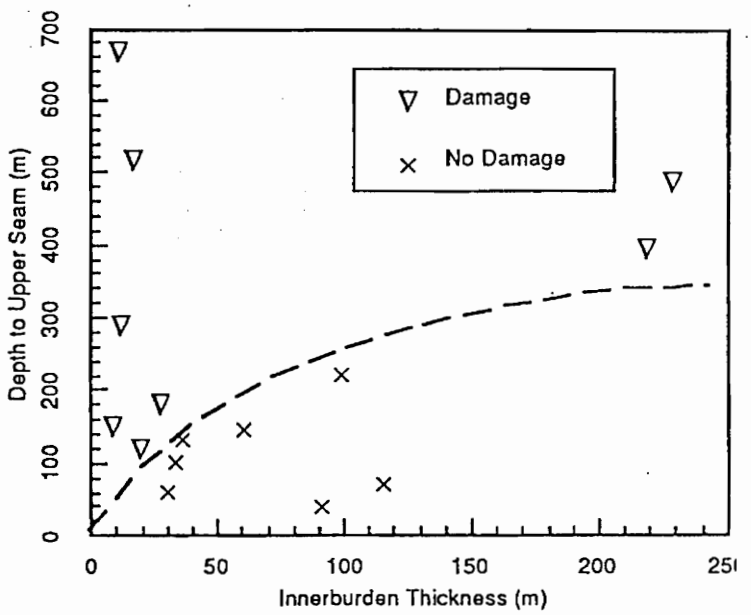

Figure 2.11 Effect of depth on stress transfer (Haycocks et al., 1992)

Some success was noted but it still lacks precision in terms of incorporating details of innerburden geology and structure. Nothing has been produced for prediction of overmining conditions.

Chapter 3

PHOTOELASTIC MODELING

3.1 Photoelasticity in Mining

Gravity loaded, low modulus, layered photoelastic methods are well suited to model strata conditions since the model properties are similar to those of strata. The multi-layer polyurethane strips can permit bed separation and interlayer slippage around openings in the prototype, simulating what happens in the mine. These phenomena, which are important for the study of ground control problems in bedded formations, are preserved in the model (Rankilor, 1968; Neall, 1975; Brady and Brown, 1985). The disadvantages of photoelastic models include such things as nonrepresentation of anisotropy of rock, effect of joints and inelastic behavior of rock (Wu, 1987).

Many researchers have successfully used photoelastic methods to study strata (Rankilor, 1968; Haycocks and Karmis, 1981; Ehgartner, 1982; Wu, 1987; Forrest, 1988). PSM-4 (urethane rubber) strips of different thickness were used for modeling layers. PSM-4 has many characteristics which make it suitable for photoelastic modeling. They are (Dally et al., 1978):

-- low modulus of elasticity

-- high sensitivity

-- low strain sensitivity

-- negligible time-edge effects

-- negligible optical or mechanical creep

3.2 Experimental Setup

The experimental setup for the studies consisted of up to 9 one-inch wide polyurethane (PSM-4) strips of different thickness. Simulation of a remnant pillar structure in an upper seam was done by loading a 1 square inch PSM-4 strip. The load was kept constant in all the experiments. To compare the stresses for each test, one reference layer was placed 1.5 inches below the experimental remnant structure/opening. A round hole was machined in the reference layer around which the stress was measured. Figure 3.1 shows the experimental arrangement.

The basic properties of the model material are given in Table 3.1. According to Obert and Duvall (1967), when static loading by gravity and linear elastic deformation are assumed, the conditions for similitude between a model and prototype are reduced to the equality of Poisson's ratio and the following equation :

$$\gamma_m l_m / E_m = \gamma_p l_p / E_p \qquad \text{-- -- -- -- -- (3.1)}$$

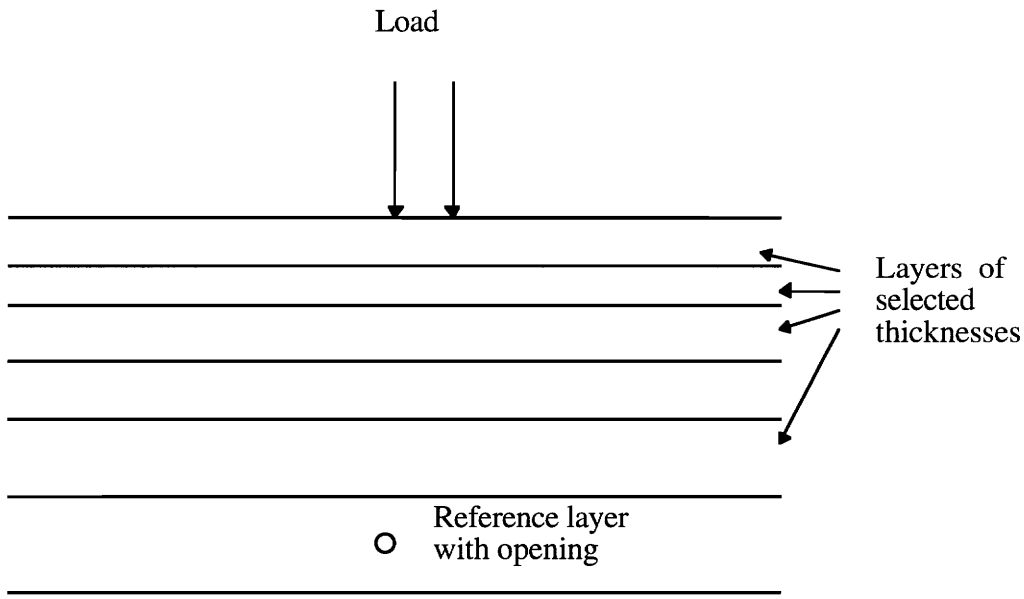

Figure 3.1 Experimental setup for the research

Table 3.1. Basic parameters of the photoelastic model and a general prototype

Properties	Unit	Prototype	Model
1. Material			
Unit Weight	kg/m^3 (pcf)	g_p=2684.4 (160)	g_m =1073.8 (64)
Poisson's ratio	--	n_p=0.3	n_m=0.5
Young's Modulus	Pa (psi)	E_p=2.58E+9 (3.75E+5)	E_m=4.13E+6 (0.6E+3)
2. Geometry			
Pillar Width	m ft(in)	W_p=12.0 40(480)	W_m=0.025 0.083(1)

Material Fringe Value of PSM-4 = 0.46 - 0.49 psi / fringe / in. (Neall, 1975)

where : γ_p, γ_m = unit weights of model and prototype;

l_m, l_p = Dimensions of model and prototype;

E_m, E_p = Young's modulus of model and prototype

From Table 3.1, we see that the linear scale of the model to the prototype is 1:480. The drawback of this material, as can be seen from the table, is that the Poisson's ratio of the model and the prototype do not match. However, in two-dimensional studies this does not materially affect the results (Fumagali, 1968).

The stress scale factor therefore becomes

$$\sigma_p / \sigma_m = \gamma_p l_p / \gamma_m l_m = E_p / E_m = 625$$

Two-dimensional photoelastic studies give a very good approximation of real situations. Coates (1965) found that when the length of the opening exceeded two times the opening width, two-dimensional studies were justified. This was corroborated by Heuze (1970), who found that there were only small changes in stress along the length in room and pillar mines.

Chapter 4

RESULTS - YOUNG'S MODULUS

4.1 Effect of Young's Modulus

To evaluate the effects of sandstones in predominantly shale innerburdens, a series of experiments were conducted. In these experiments the effect of changing Young's Modulus in selected layers was evaluated in terms of stress transfer to layers below. The magnitude of the stress was studied at the following locations :

1) above the experimental layer
2) below the experimental layer

Figure 4.1 shows the experimental setup. Figure 4.2 shows the effect of Young's Modulus of the layer on the magnitude of stress for the two cases which exhibited different behavior. The layer content was constant at 18% as shown in Figure 4.1. Young's Modulus was studied as a ratio rather than as an absolute quantity, because it was thought that the correlation to real life sandstones and shales could be made more easily with ratios rather than with specific values. For the first situation modeled, the stress was measured above the experimental layer (above the layer) and it was seen that as the Young's Modulus increased, the stress magnitude decreased. Thus, it was concluded that for a high modulus layer, the magnitude of stress *above* the layer will be less than that for a low modulus layer. For the stresses below the layer, the

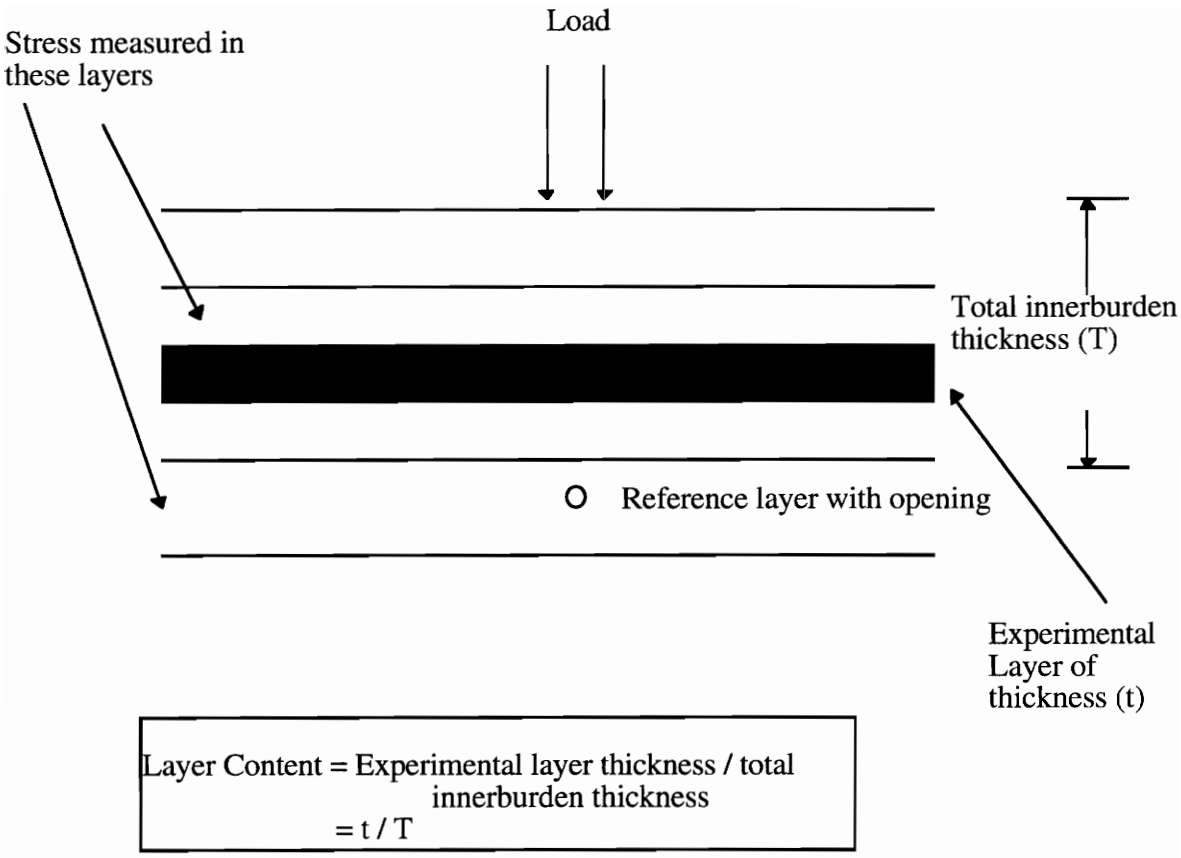

Figure 4.1 Experimental setup to study the effect of Young's Modulus

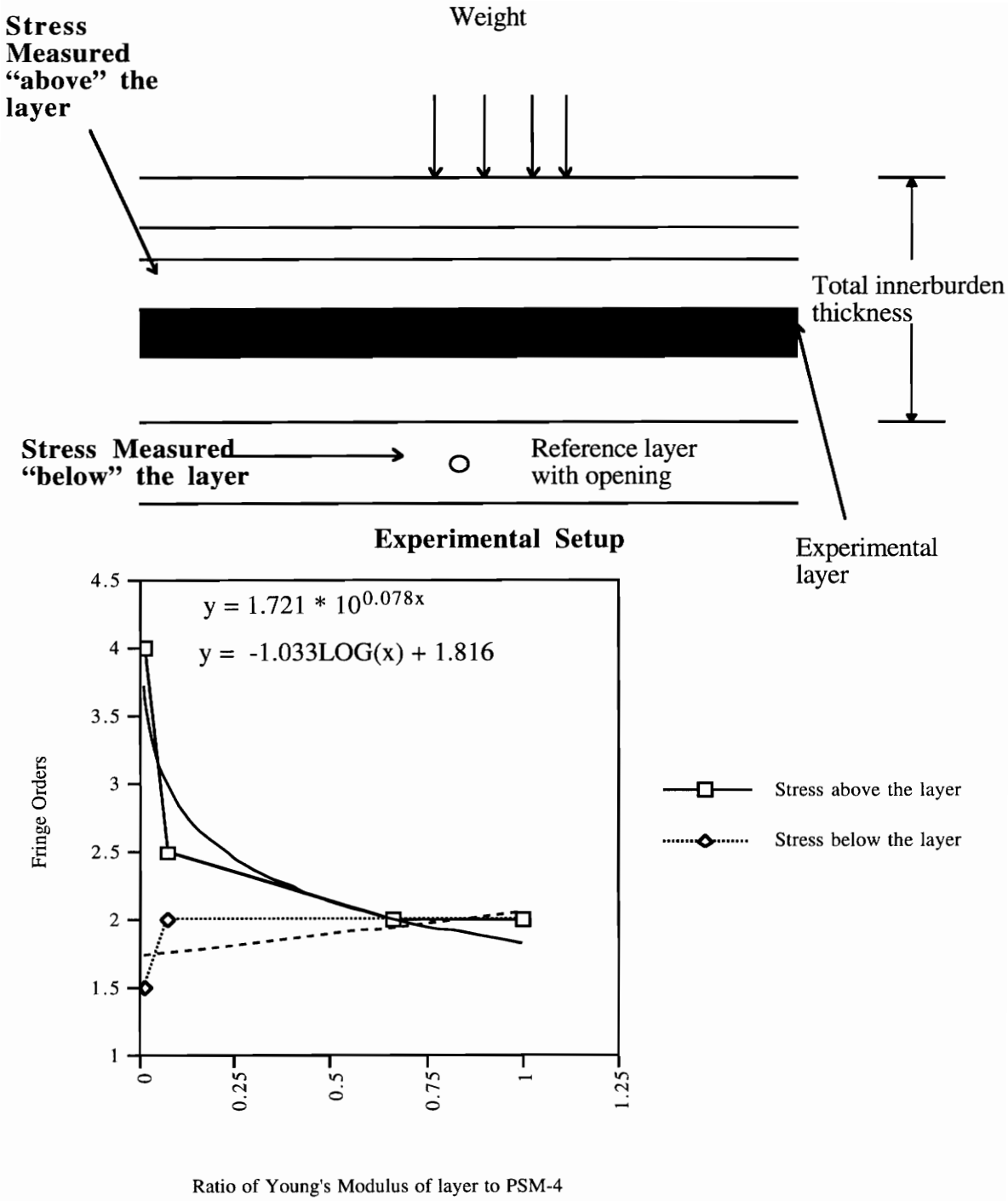

Figure 4.2 Stress variation both above and below experimental layer, with Young's Modulus, at 18 % experimental layer content.

behavior was opposite to that observed in the overlying strata as can be seen from Figure 4.2. As the layer modulus was reduced, less stress was transferred to the reference layer below. Based on these observations it was concluded that low modulus layers transfer less stress to strata below even though the stress above the layer is higher. For layers of very high modulus, there is very little or no transfer of stress. For example, when a steel layer was introduced, there was no discernible stress transfer to the layers below.

To investigate the effect of thickness of layers on Young's Modulus, the above factors were studied at different layer thicknesses (or different layer content percentages). This was done by progressively increasing the thickness of each layering. Figures 4.3 and 4.4 show the stresses at 36% and 54% layer content respectively. As the thickness of the low modulus layer increased, the stress above the layer increased. With the increase in thickness of a low modulus layer, there was less transfer of stress to strata below. Figure 4.5 summarizes the effect of Young's Modulus of layering on stress above the layer. A decreasing trend of stress with increasing Young's Modulus is evident. Figure 4.6 summarizes the effect of Young's Modulus of layering on stress below the layer. In this case, an increasing trend of stress with increasing Young's Modulus is evident. In the former case (Figure 4.5), increasing thickness serves to increase the stress while the opposite is true in the latter case (Figure 4.6). To facilitate a comparison of these findings, Figure 4.7 compiles all the trends.

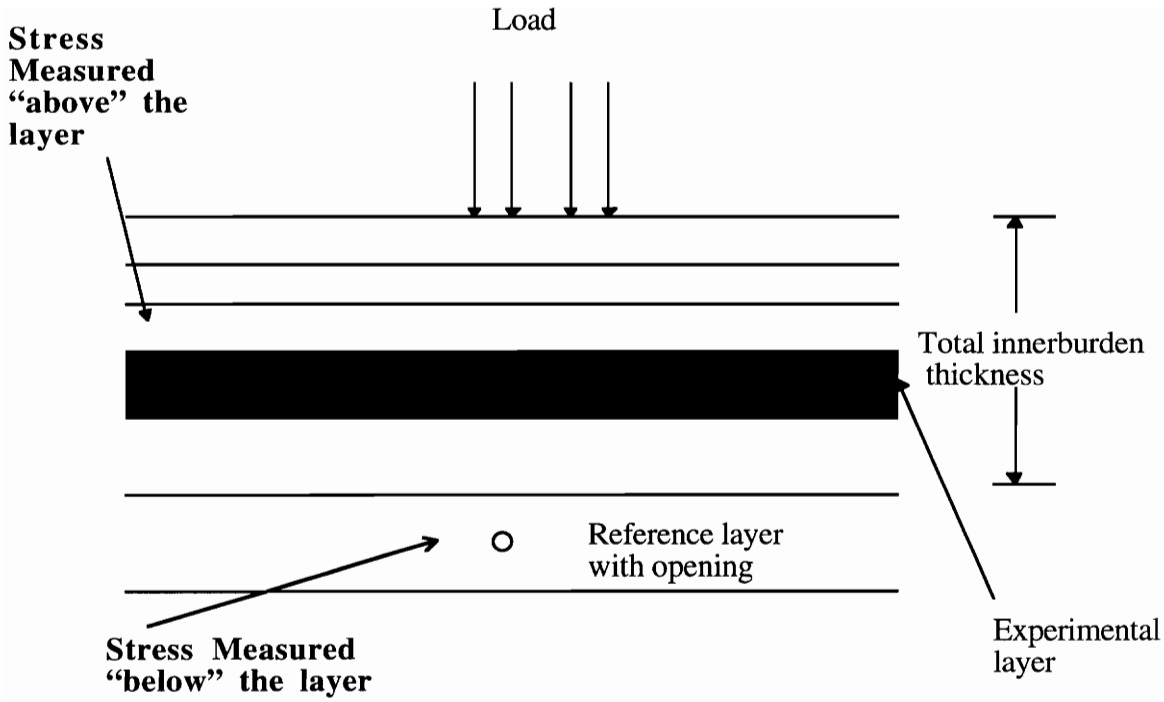

Experimental Setup

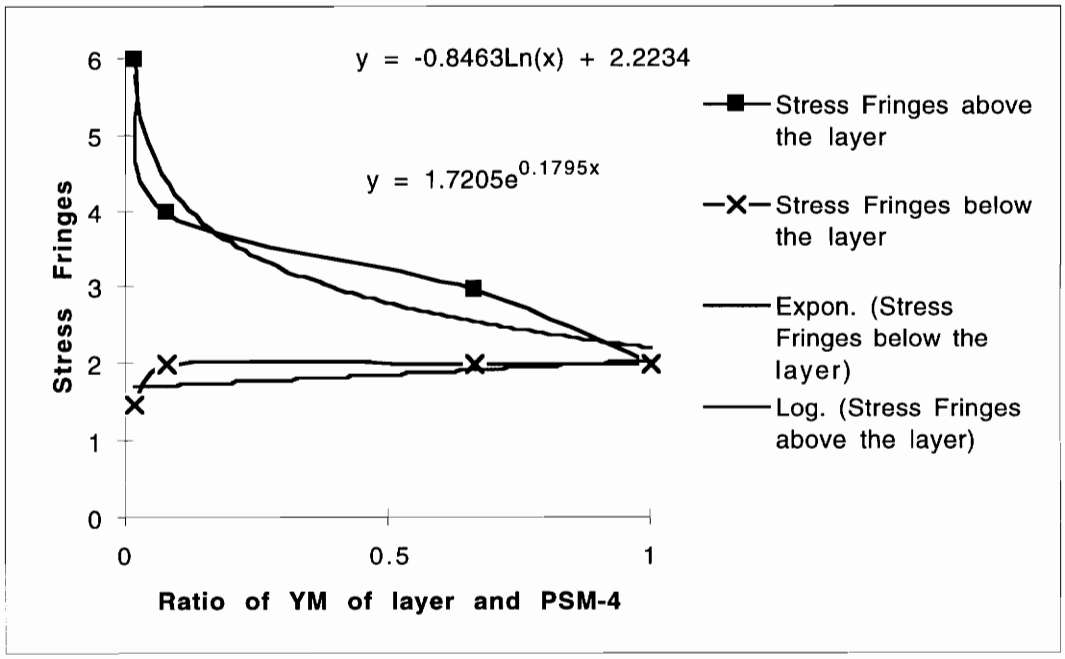

Figure 4.3 Stress variation both above and below experimental layer for changes in Young's Modulus, at 36% experimental layer content.

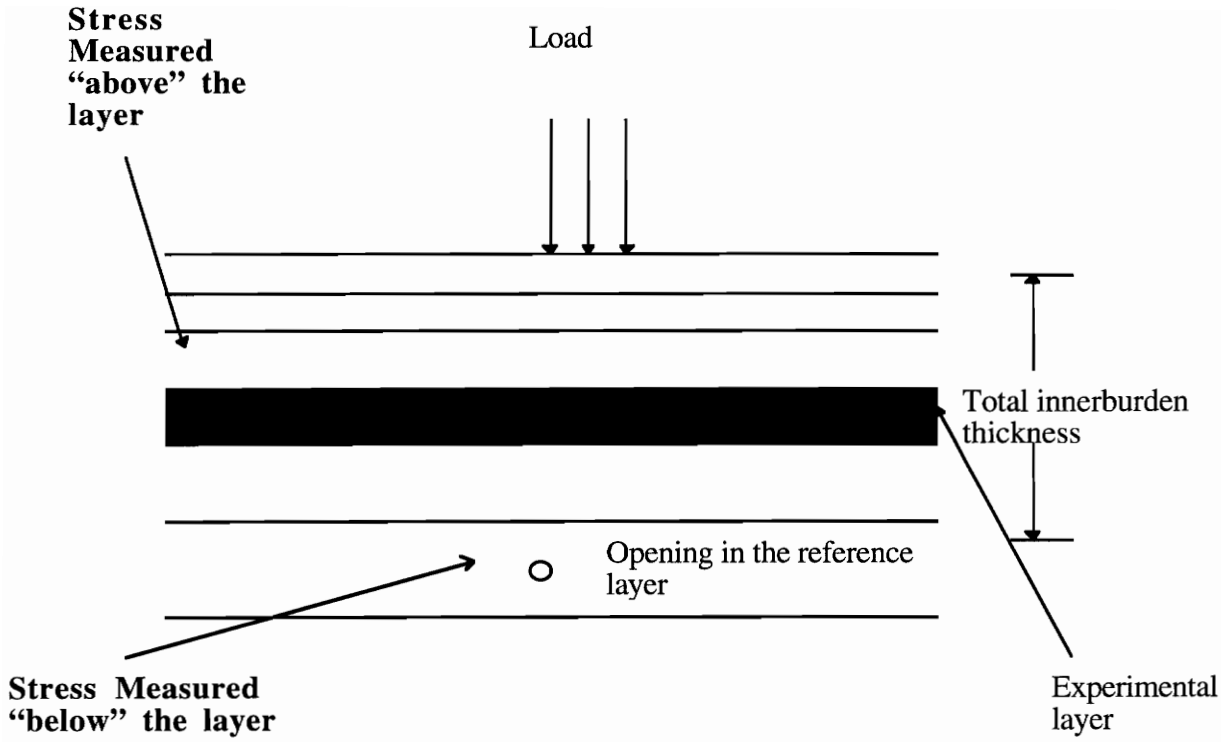

Experimental Setup

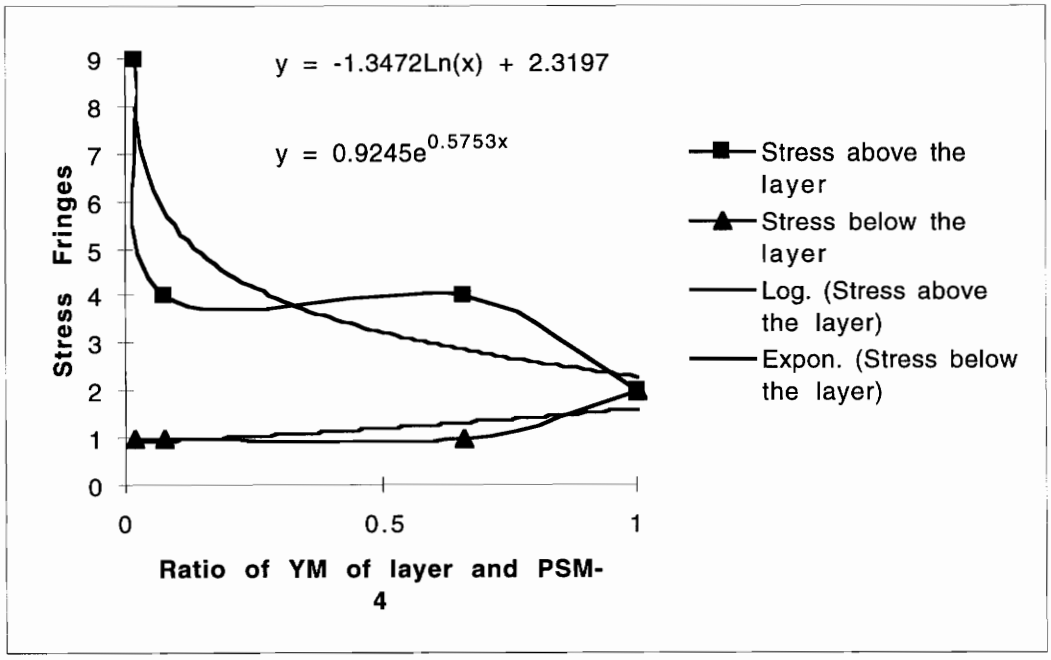

Figure 4.4 Stress variation both above and below experimental layer for variations in Young's Modulus, at 54% experimental layer content.

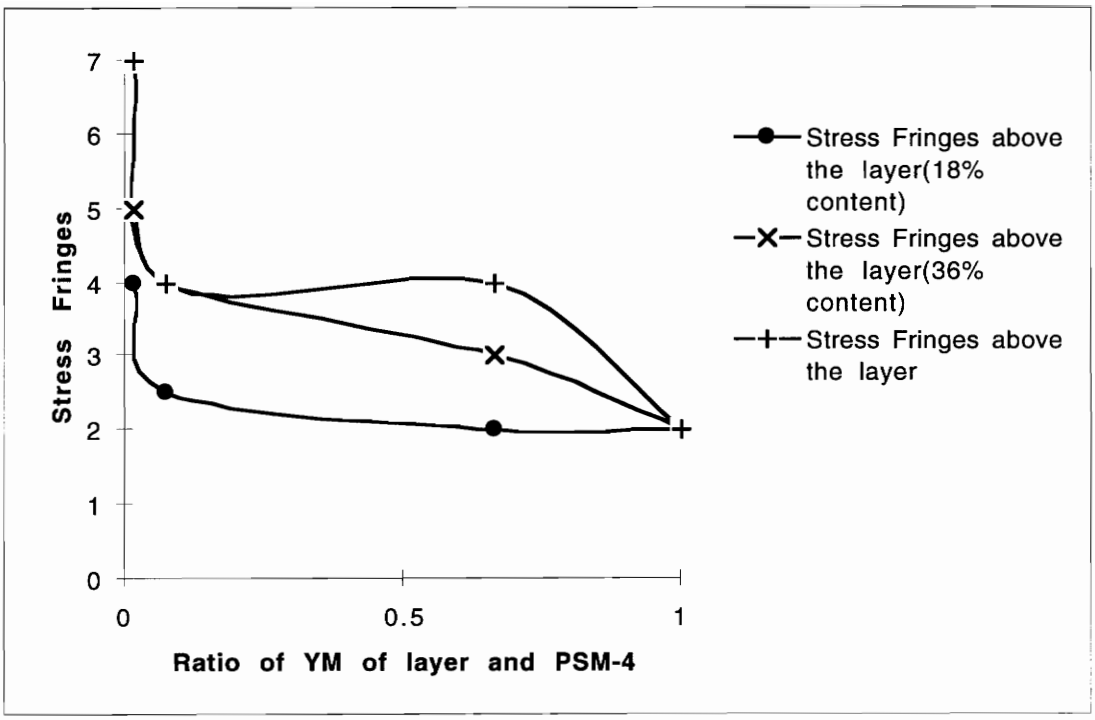

Figure 4.5 Variation of Stress with Young's Modulus in the layer *above* as the content of experimental layer changes

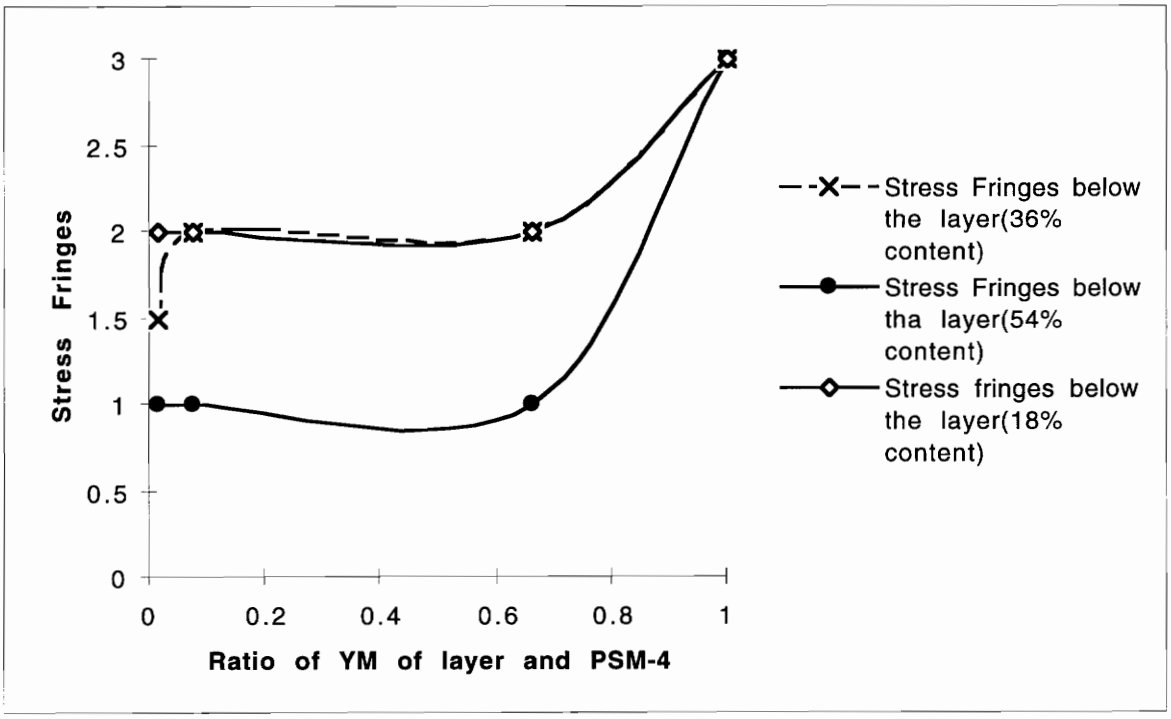

Figure 4.6 Variation of Stress with Young's Modulus *below* the layer, as layer content changes

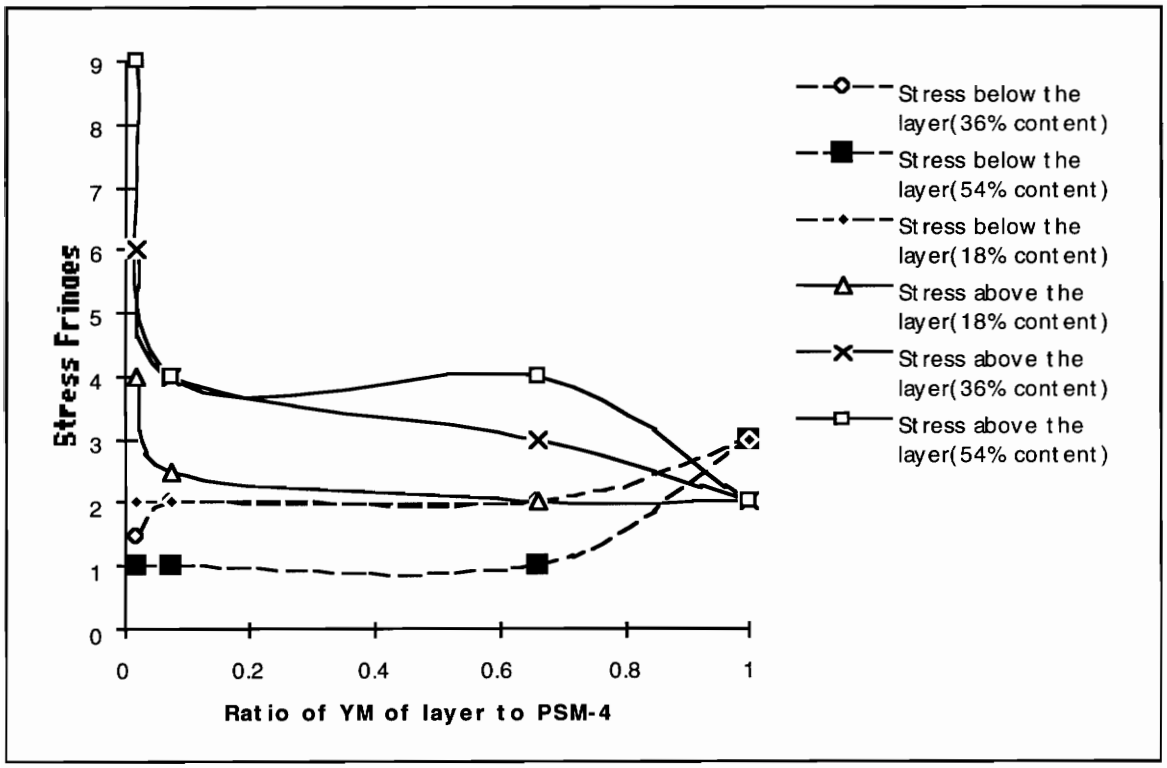

Figure 4.7 Variation of Stress with Young's Modulus for variations in the location of the layer and content

The trends of the stress level *above* the layer were found to follow a logarithmic distribution. It can be seen that the latter part of all the curves is linear. Some typical values of Young's Moduli for coal bearing strata are given in Table 4.1. Hence, in actual mining situations, the ratios are more likely to be as in the latter linear part of the curves. Between the ratios of 0.1 and 1 it can be seen (Figure 4.5) that the highest stress can be up to one and a half to two times the lowest stress. In other words, *if we have a low modulus layer and a high modulus layer under similar conditions, the stress above the low modulus layer will be one and a half to two times the stress above the high modulus layer, depending on the thickness of the layers.* It should be remembered, however, that for a layer with a very high modulus with a large overburden, the layer above may be squeezed, in which case, the stresses will be very high. For actual mining conditions, where the ratios are between 0.25 and 1 (as in the latter part of the curves), Young's Modulus seems to have little effect on the stresses for low layer contents (36% and below).

The stress *below* the layer was found to follow an exponential distribution. Similar to the case cited earlier, the latter part of the curves is linear. Thus, for actual mining conditions we can assume linear distribution of stresses below the layer. In this case, we see that the stresses can be two to three times the lowest stress for the high stress conditions. The difference is that the stresses are low for low modulus layers, unlike the former case.

Table 4.1 Typical Young's Moduli for coal bearing strata*

Rock Type	Young's Modulus N / m^2(psi)
Coal	3.45 E +9 (5E +5)
Sandstone	12.4 E +9 (18E +5)
Siltstone	1500000
Shale	940000

* Akram, 1993.

In other words, *if we have a low modulus layer and a high modulus layer in similar conditions, the stress below the high modulus layer will be two to three times the stress below the low modulus layer, depending on the thickness of the layers*. Transfer of stress is less for low modulus layers than for high modulus layers. Again, for actual mining conditions where the ratios are high (between 0.25 and 1), Young's Modulus has very little effect on stress transfer for low layer contents (36% and below).

High lateral spread of stress was seen in the PSM-4 layers above the experimental low modulus layers. Since the experimental layers in these cases were not made of photoelastic material, the stress pattern was not visible in them. However, they can be assumed to follow the same pattern as seen in the layers above. Hence, it can be said that layers of low Young's Moduli tend to laterally spread the vertical stresses and have high lateral spread. This is similar to the observations made by Ehgartner (1982). The same is also shown in the literature review in Figure 2.3.

Regarding the nature of the observed stresses, the individual layers behaved as loaded beams with tensile stresses at the bottom of each layer and compressive stresses at the top. When a high modulus layer is present, the deformation of the layers above it is restricted and hence the stresses are minimized. Low modulus layers are compressed under stress and hence the stress energy, instead of being transmitted, is absorbed by the layer. This is similar to the way crash helmets work, wherein the helmet absorbs the energy

of the crash using it for shattering rather than transferring the energy to the head. This explains why stress below low modulus layers is reduced.

Finite element studies were also conducted to examine the effect of Young's Modulus on stress transfer. Finite element code UTAH2PC was used for the purpose. The model had five layers, each five elements thick. The Young's Modulus of the middle layer was varied for the purpose of the computer simulations. The stress above and below this layer was determined by the model. It was found that the severity of stress transfer, as produced in finite element studies, was less than in the photoelastic studies. This is because the finite element method assumes perfect bonding between layers.

The presence of tensile and compressive stresses at the bottom and top of each layer was not evident in the finite element studies. This was due to the absence of any slippage between layers without which prototype conditions are not effectively modeled. The whole mesh is one single entity, and thus, in this method only compressive stresses, with magnitudes decreasing in the vertical direction, are seen. It should be pointed out that the magnitude of compressive stress diminishes in the horizontal direction as the nodes get farther from the load. Figure 4.8 and 4.9 show the finite element output. Examples of low and high modulus material can be found in Table 7.1.

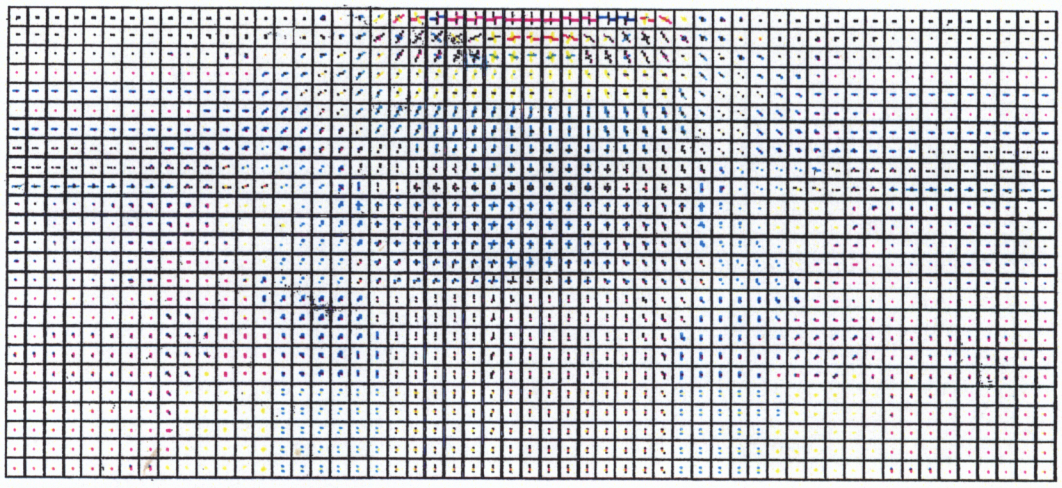

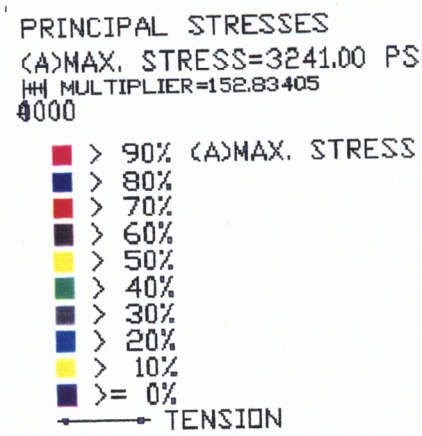

Figure 4.8 Finite Element Output with low modulus layer in the middle

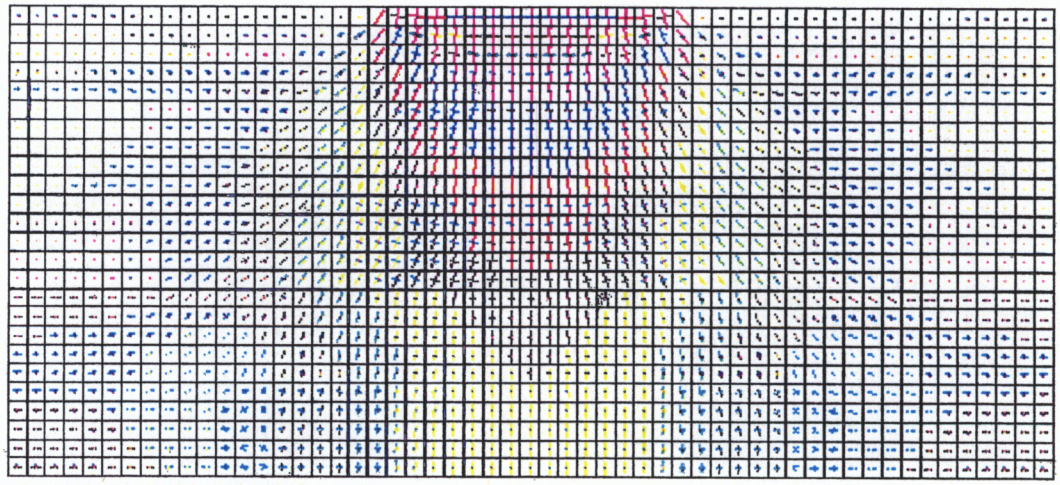

LOADING THE MESH WITH LOAD.

PRINCIPAL STRESSES

(A)MAX. STRESS=2069.00 PS

+++ MULTIPLIER=78.05336

04000

- > 90% (A)MAX. STRESS
- > 80%
- > 70%
- > 60%
- > 50%
- > 40%
- > 30%
- > 20%
- > 10%
- >= 0%

TENSION

Figure 4.9 Finite Element Output with high modulus layer in the middle

Chapter 5

RESULTS - OTHER PARAMETERS

5.1 Effect of Thickness of Layer

Layer thickness has been previously shown to affect stress transfer. Experiments were conducted to study the precise mechanism of stress transfer and to determine if methods of prediction can be developed.

Photoelastic layers of varying thickness were loaded and the maximum lateral spread of stress was noted for each thickness. Figure 5.1 shows the experimental setup. Figure 5.2 shows the effect of thickness on stress transfer for a load of 3.13 psi. It is clear from this latter figure that thickness increases the lateral spread of stress and that the variation is linear for the early part of the curve. The spread decreases following a peak in stress. This happens because as the thickness increases, the stress cannot be sustained over a large area and this is reflected in a decrease in lateral spread of the pressure bulb. The variations for different stress levels are similar for the same layer thickness and applied load. For the same load and thickness, as the stress level increases the spread decreases. Figure 5.2 clearly demonstrates the phenomenon. It can be seen that the curve for fringe order-2 is below that of fringe order-1, or while the variation is similar, the magnitudes are less.

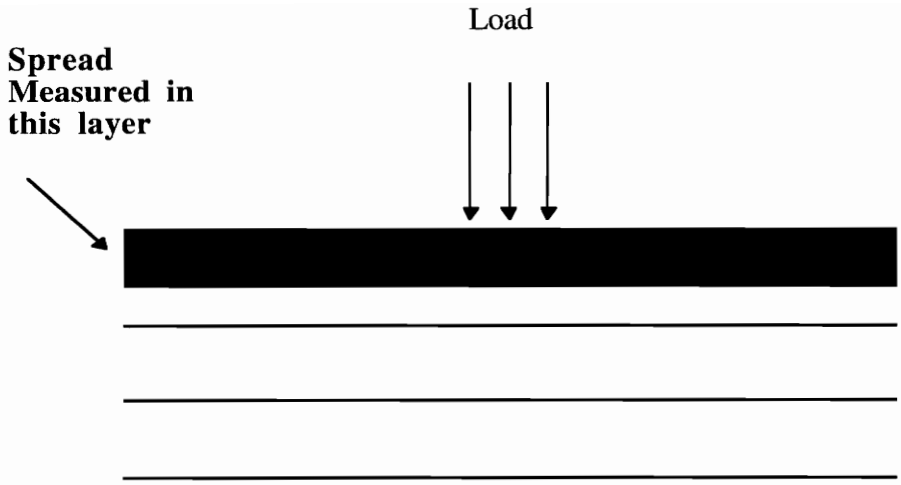

Note :

Experiments were conducted at constant loads for different layers.

Different sets of experiments were conducted at different loads to study the effect of load. Each set of experiments had a constant load but the thickness varied.

Figure 5.1 Experimental setup to study the effect of thickness on lateral spread

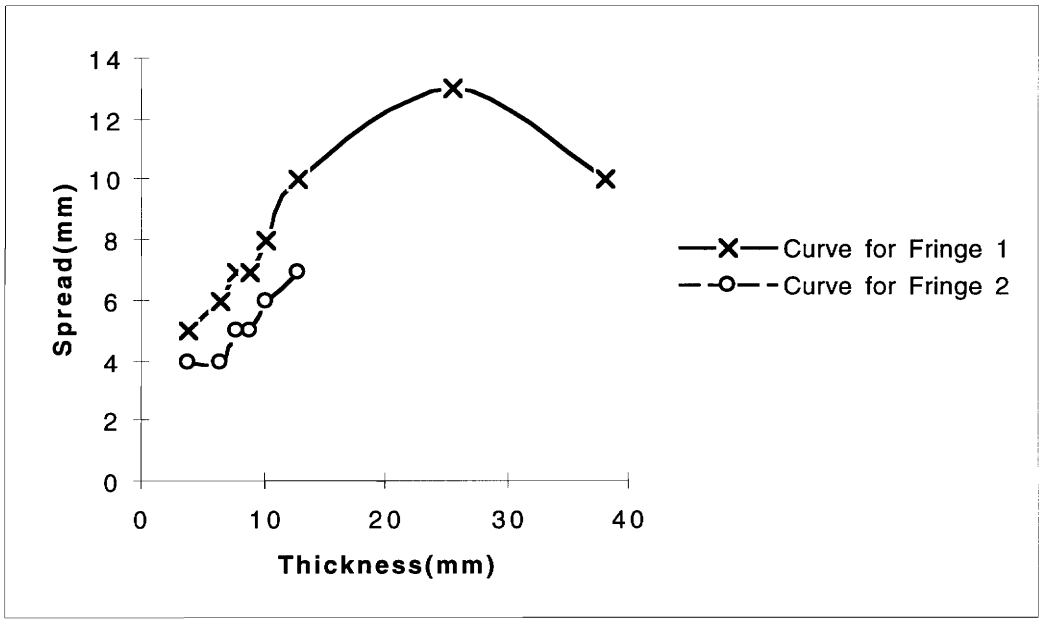

Figure 5.2 Effect of thickness of layer on lateral spread of stress for 3.13 psi

The data for fringe order-2 is minimal. This is because as the thickness increased from 0.5 inches to 1 inches, it ceased to exist. Fringe order-1 corresponds to a stress of 0.49 psi and fringe order-2 corresponds to 0.98 psi. The material fringe value of PSM-4 is 0.49 psi / fringe / inch (Neall, 1975).

It should be noted, however, that as the load increases, lateral spread will also increase for the same thickness and stress level. Figures 5.3 and 5.4 show the thickness - displacement relationship for different loads (2.51 psi and 5.64 psi, respectively). The displacements, in this case, are higher for the same stress level, at higher loads and less for less loads. This is clearly evident in Figure 5.5 where the lateral displacements for fringe order-1 have been plotted for various loads. For a specified load, however, lateral spread of stress and layer thickness have an initial linear relationship, depending on the magnitude of the load. For higher loads, the linear portion is extended up to a greater thickness. It should also be noted that fringes of higher order will have a smaller linear portion than fringes of lower order, for the same load. This is because the strata dissipate higher stresses.

To summarize, the effects of thickness, load and stress level on lateral spread result in the following:

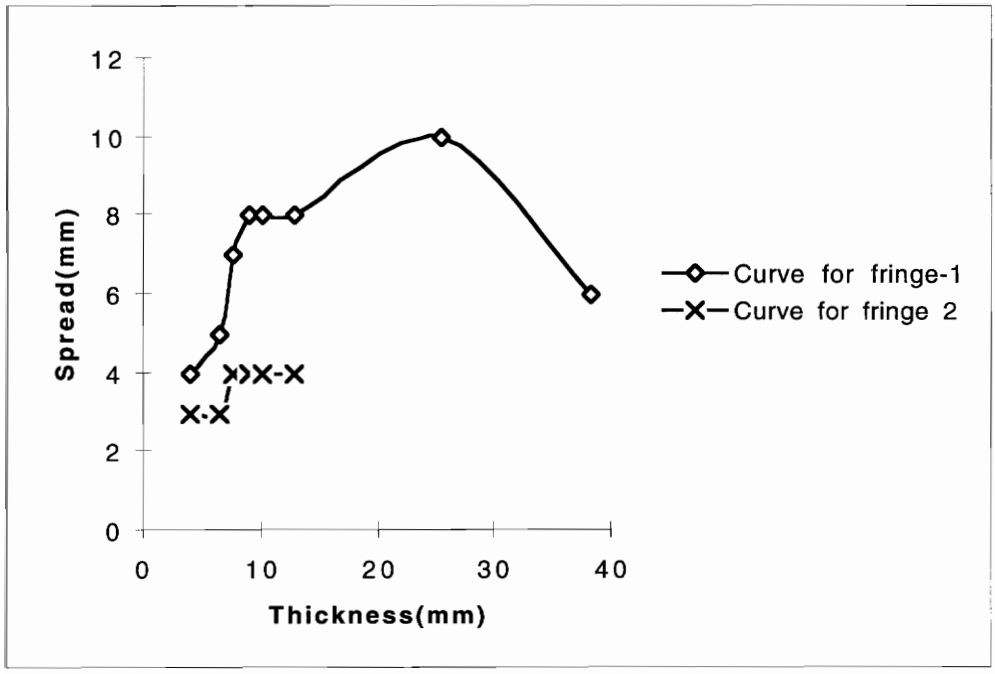

Figure 5.3 Effect of thickness on lateral spread of stress for 2.51 psi

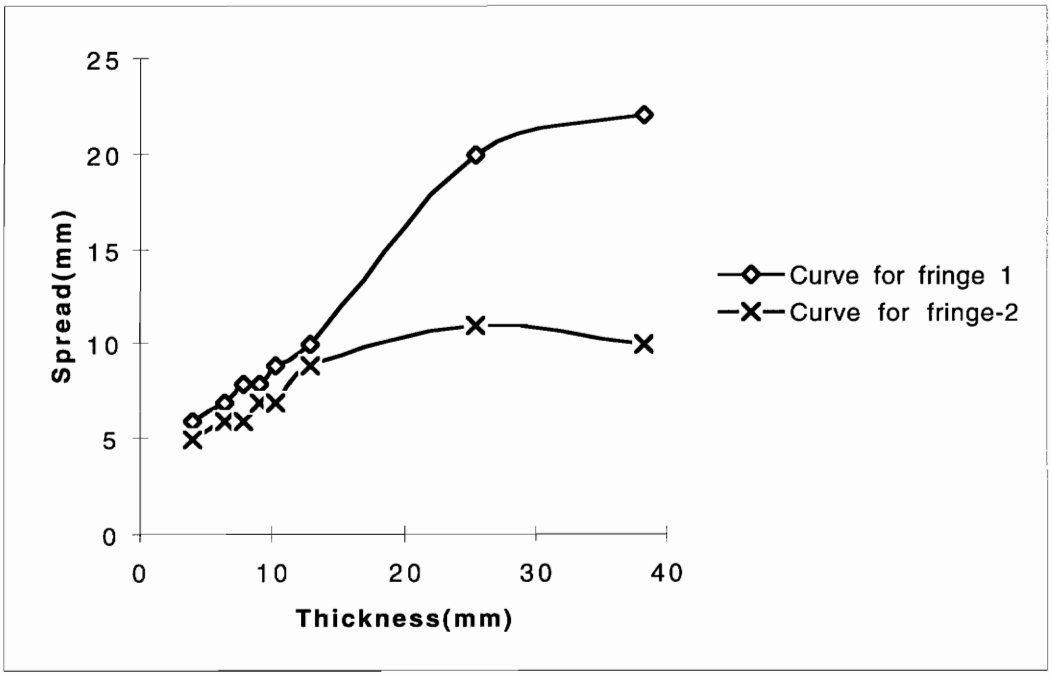

Figure 5.4 Effect of depth and thickness on lateral spread of stress for 5.64 psi

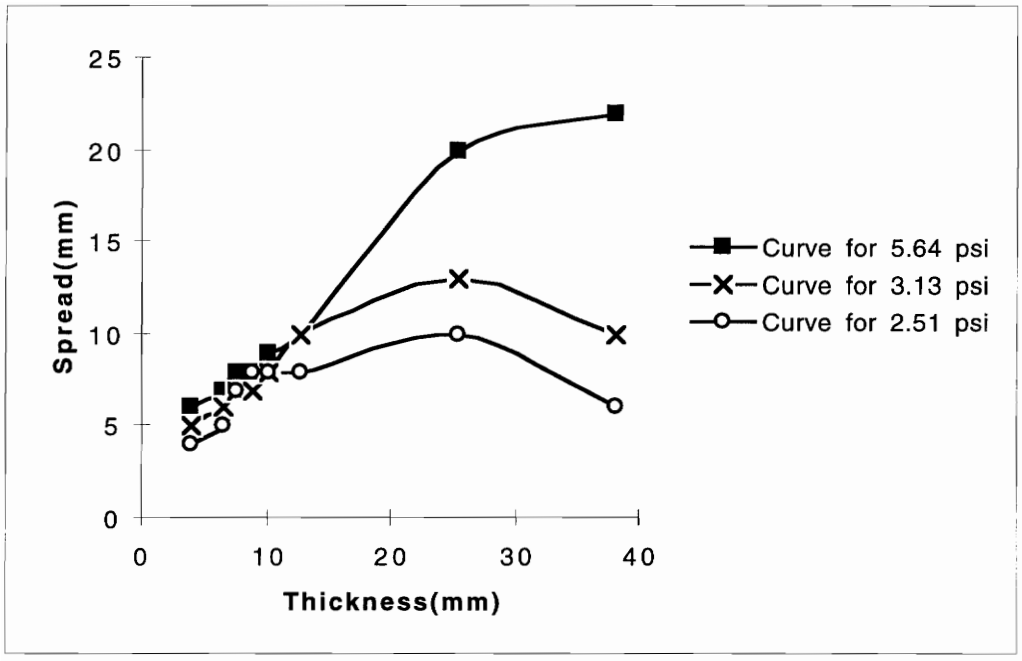

Figure 5.5 Variation in lateral spread with load and thickness

For constant thickness and load

i) As the stress level increases, the spread decreases.

For constant thickness and stress level

ii) As the load increases, the spread increases.

For constant load and stress level

iii) As the thickness increases, the spread increases linearly at first and after flattening out, it decreases. The rate of change of spread with thickness would also depend on the Young's Modulus of the layer.

iv) The linear portion of the curve depends on the load, and increases with increasing load.

While the above series of experiments was carried out on layers which were loaded directly, the following series of experiments was made on layers simulating different depths (Figure 5.6). It is known that below a certain depth the stress bulbs curve inward. This is due to the influence of depth and thickness. Thus, the effect of thickness and depth together on the lateral spread required investigation. The thickness and depth were studied as the ratio of depth to thickness changed.

The thickness was varied from 0.15 inch (3.81 mm) to 0.5 inch (12.7 mm). For each thickness, the layers were placed at different depths and the lateral spread of stress was measured. When the experimental layer was the first layer (or when the depth was zero), the displacement was measured from the edge of the pillar. For other depths, only the increase or decrease of lateral spread was

measured. This was done in reference to the lateral spread of stress in the layer above. It was observed that since thin layers do not spread the stress laterally, if the experimental layer had a thin layer above it, an increase in lateral spread of the stress in the experimental layer was always observed, regardless of the depth. Conversely, thick layers above the experimental layer caused a decrease in lateral spread of stress. To overcome this problem, a layer of constant thickness (0.3 inch or 7.62 mm) was always placed above the experimental layers.

Two series of tests were carried out. The first set was simple, with innerburden totaling 1.5 inches as shown in Figure 5.6. The results of these tests were termed "without opening in the bottom layer". The second set is given in Figure 5.7 and has a reference layer at the bottom. The results from these tests were termed "with a hole in the bottom layer." The bottom reference layer did not constitute the innerburden. Figure 5.8 explains the various terms used in this series of experiments.

Figure 5.9 shows the curve of displacement against ratio of depth to layer thickness, drawn for a 0.15 inch layer. Variation has been plotted for Fringes 1 and 2. Fringe -1 corresponds to a stress level of 0.49 psi or 0.16 times the loading stress. Fringe-2 corresponds to a stress of 0.98 psi or 0.32 times the loading stress. It can be seen that at zero depth there is a spread of 4 mm (for Fringe-1). The ratio of zero means that the *depth is zero* or *the layer is directly loaded* by the remnant structure. As the depth increases to 0.3 inches or the

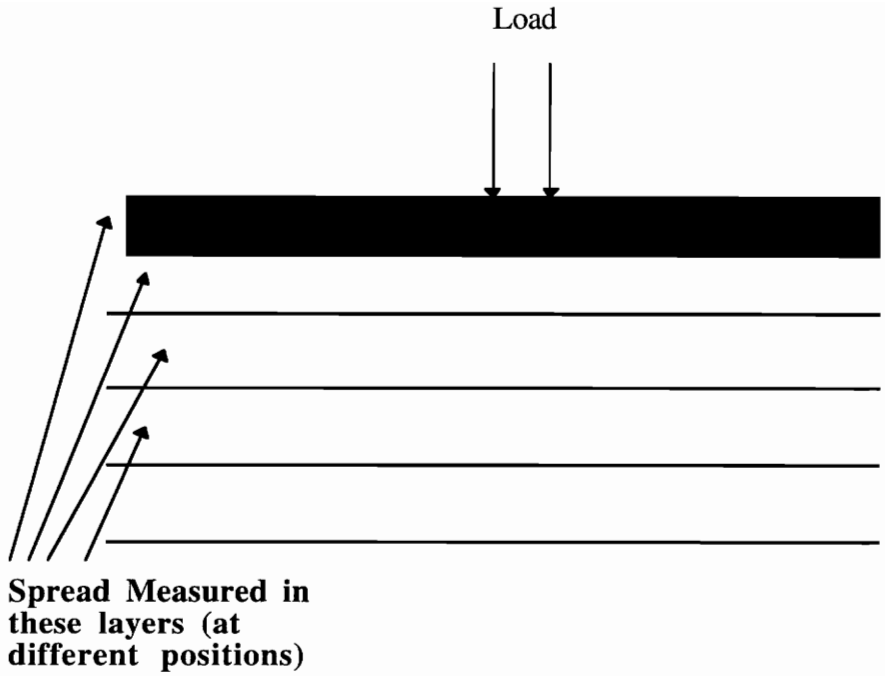

Note :

Each set of experiments consisted of a layer of constant thickness placed at different depths. The lateral spread was measured in each case.

Different sets consisted of layers of different thickness. In each set the layer thickness was constant.

These experiments had no reference point in the bottom layer. The results from these tests were termed as "without hole in the bottom hole."

Figure 5.6 Experimental setup to study the effect of layer thickness and depth on lateral spread (without opening in the bottom layer)

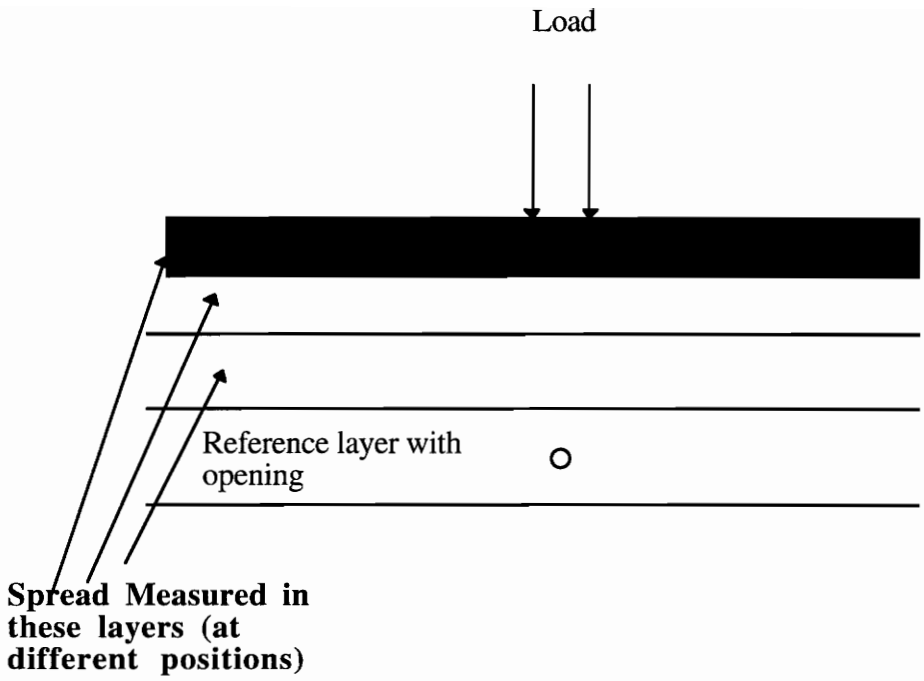

Note :

Each set of experiments consisted of a layer of constant thickness placed at different depths. The lateral spread was measured in each case.

Different sets consisted of layers of different thickness. In each set the layer thickness was constant.

Since the bottom reference layer had a hole in it, the results were termed as "with hole in the bottom layer". The bottom reference layer did not constitute the innerburden.

Figure 5.7 Experimental setup to study the effect of layer thickness and depth on lateral spread (with opening in the bottom layer).

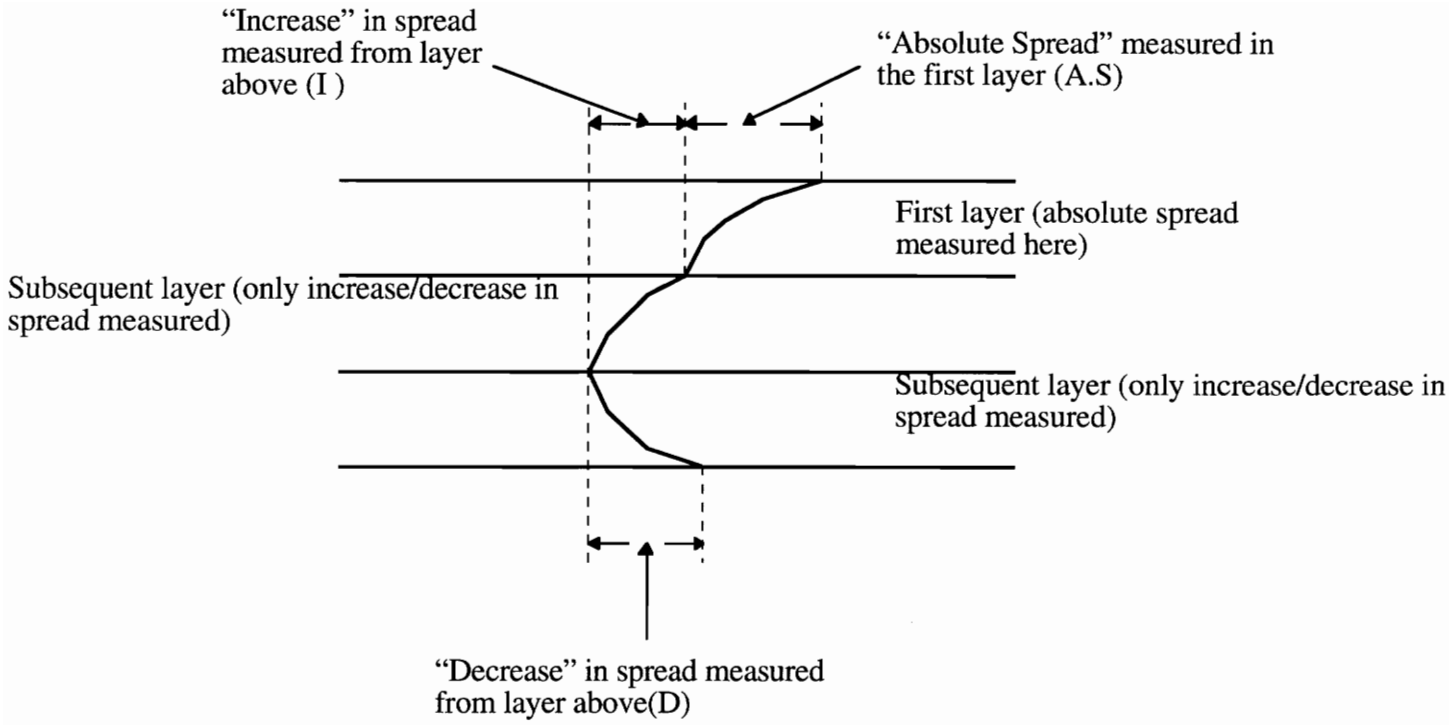

Notes :

1. When the experimental layer was the first layer, the absolute spread was measured as shown above.

2. When it was any of the subsequent layers, only the increase or decrease in spread (whichever appropriate) from the layer above was measured.

3. Cumulative spread is the sum of the absolute spread and all subsequent increases or decreases (decrease is negative increase in spread) in spread.

Cumulative Spread = A.S + I - D

Figure 5.8 Explanation of terms used in the experiment.

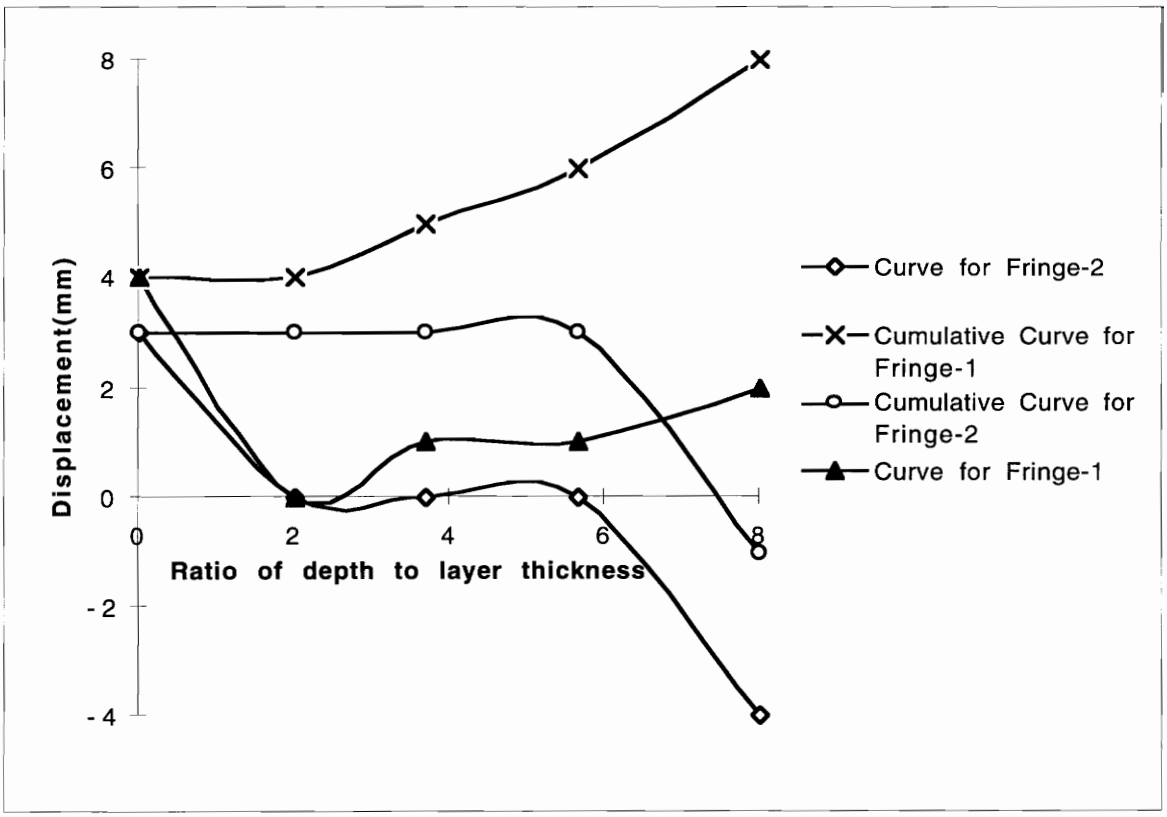

Figure 5.9 Effect of depth and thickness on lateral spread of stress for 0.15 inch layer, without an opening in the bottom

ratio becomes 2, the spread remains unaffected. This is reflected by a zero increase in spread. It should be remembered that for zero depth the absolute spread was measured, whereas for other depths, the *increase/decrease* was measured. For further increases in ratio it can be seen that the increase is steady at 1 mm. At a ratio of 8, however, there is a sharp increase in spread. Also plotted were the cumulative curves for Fringes 1 and 2. The total spread was cumulatively added for each fringe order. This gives an indication of the shape of the pressure bulb. This shape would approximately resemble the shape of the pressure bulb if all the layers were 0.15 inches thick. The steady increase in spread is clearly evident. For fringe order-2, however, the variation is different. There is little or no change in spread up to a ratio of 6, after which there is a sharp decrease in spread.

Figures 5.10, 5.11 and 5.12 show the variations for 0.25, 0.30 and 0.50 inch layers respectively. The increases are similar, with the spread for fringe order-1 being more than that of order-2. It is also evident that spread depends on the Young's Modulus, too. From the curves it can be seen that up to a ratio of 4, the spread (for Fringe -1) increases except for the layer of thickness 0.50 inch, for which the plot exists up to only 1.75. It must be remembered that since these are ratios of depth and thickness, the same ratio for two thickness means different depths, with a larger depth for the thicker layer.

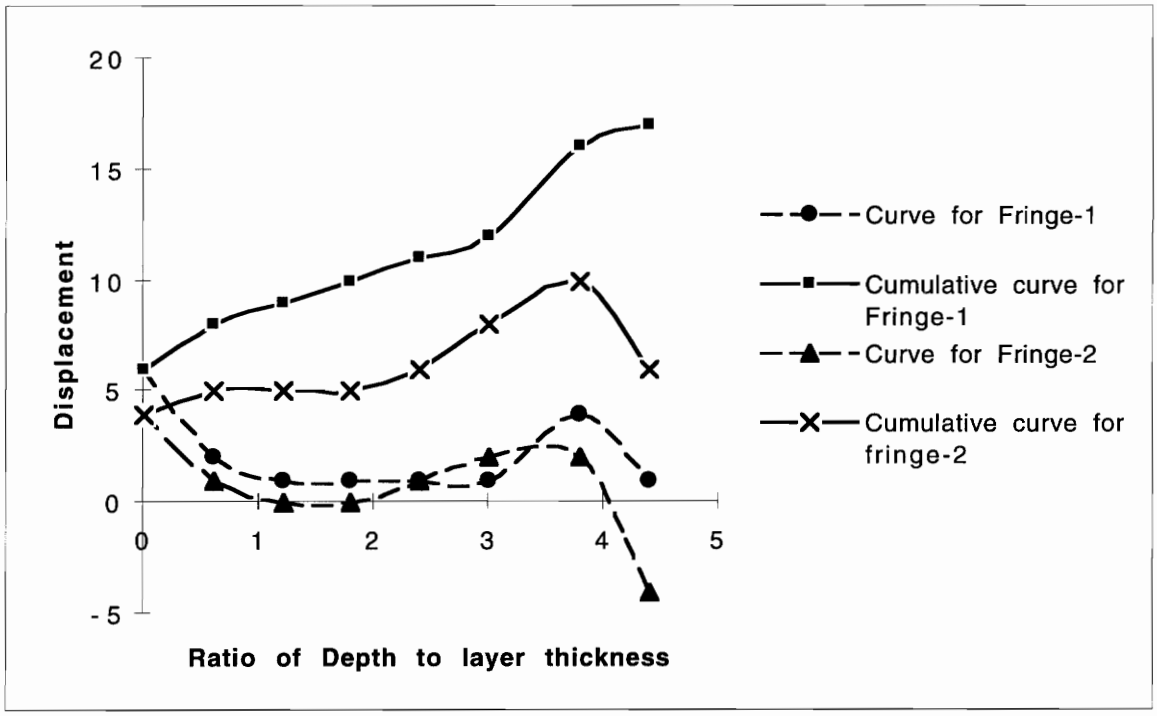

Figure 5.10 Effect of depth and thickness on lateral spread of stress for 0.25 inch layer (without opening)

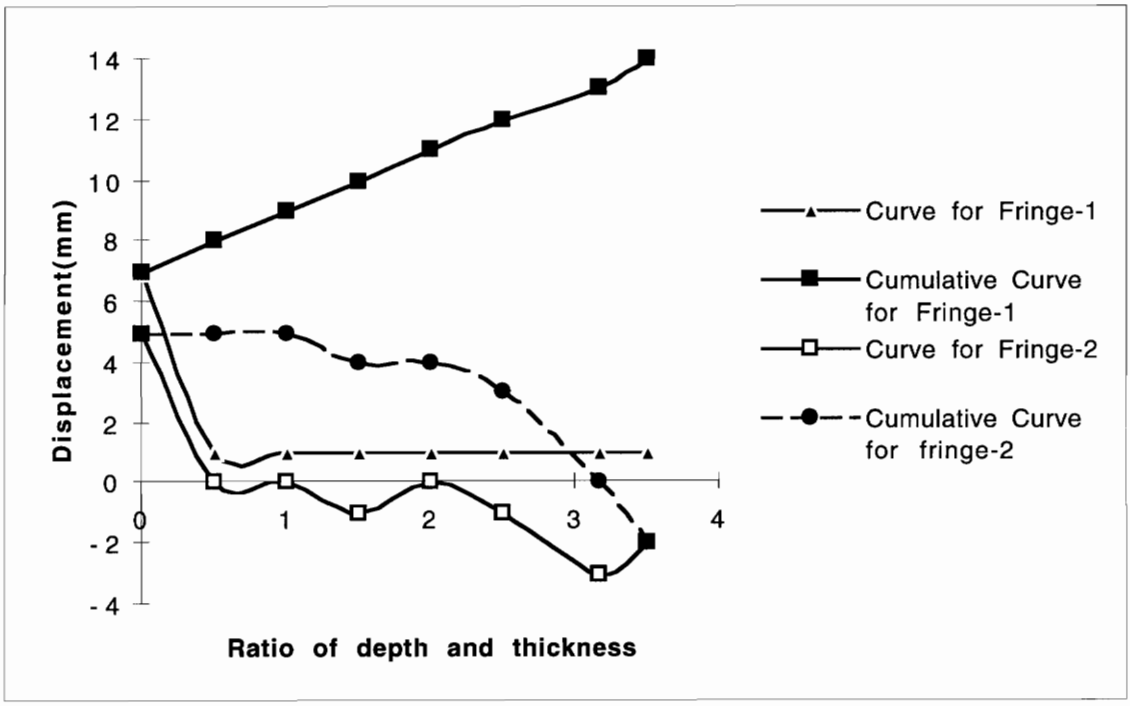

Figure 5.11 Effect of thickness and depth on 0.3 inch layer (without opening)

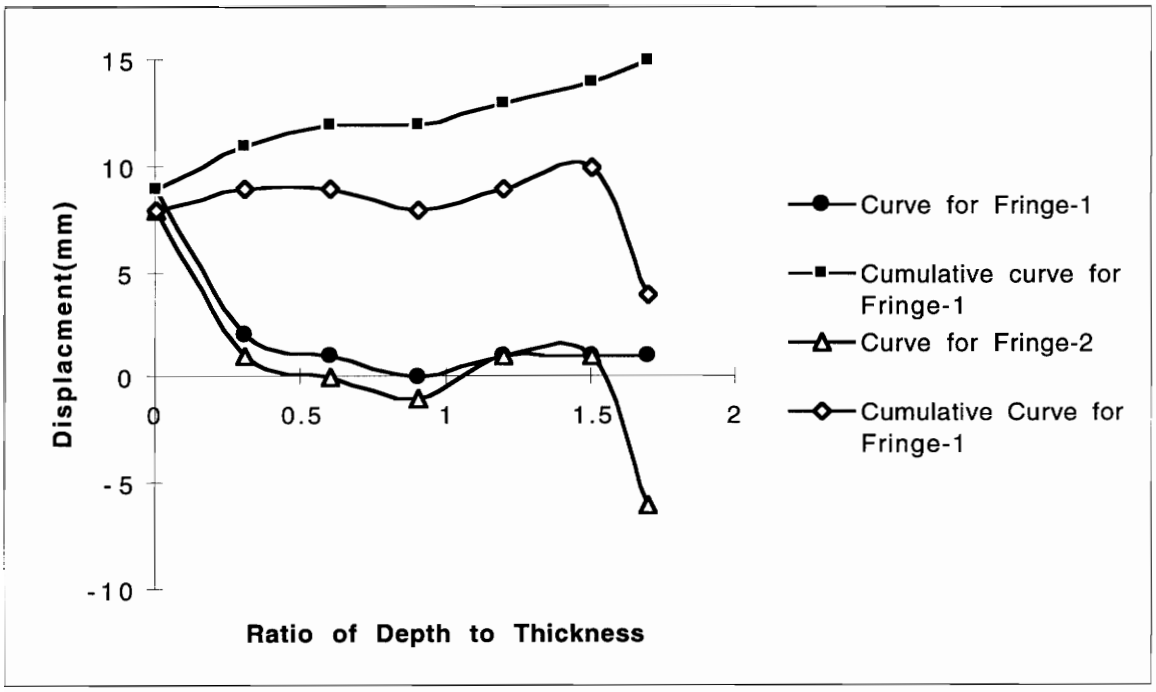

Figure 5.12 Effect of thickness and depth on lateral displacement in a 0.5 in layer - without an opening

The increase would be less, for the same ratio, in the case of thick layers since the stress would dissipate at greater depths.

From Figures 5.9, 5.10, 5.11 and 5.12 it can be seen that the absolute depths (not ratios) at which the spread of the fringes changes direction from increasing to decreasing, decreases with increasing thickness. This suggests the effect of thickness on stress transfer. For 0.15 inch layer thickness, fringe order-1 has a steady increase up to a ratio of 8 (or 1.2 inch depth). Fringe order-2 changes direction at a ratio of 6 (or depth of 0.9 inches). For 0.25 inch layers the values are 1.0 inch and 1.0 inch (fringe-1 and fringe-2). For 0.50 inch, the values are 0.85 inch and 0.75 inch, respectively. There are more layers present for the same depth for thin layers than for thick layers. Hence, it is seen that stress increases spread up to a greater depth for thin layers than for thick layers. Thick layers tend to dissipate stress.

The next series of experiments was conducted where the bottom layer served as the reference layer. This layer had a hole in the center for ease in stress measurement. Figures 5.13, 5.14, 5.15 and 5.16 show the relationship between spread of stress and ratio of depth to thickness. The effect of the reference hole is very evident from the curves. Instead of a decreasing spread with depth, it can be seen that the spread increased after a critical depth had been reached. This occurred because the deeper the layer in the model, the closer it was to the hole in the reference layer. This caused the stress to flare outward rather than inward, due to the effect of the pressure arch over the small

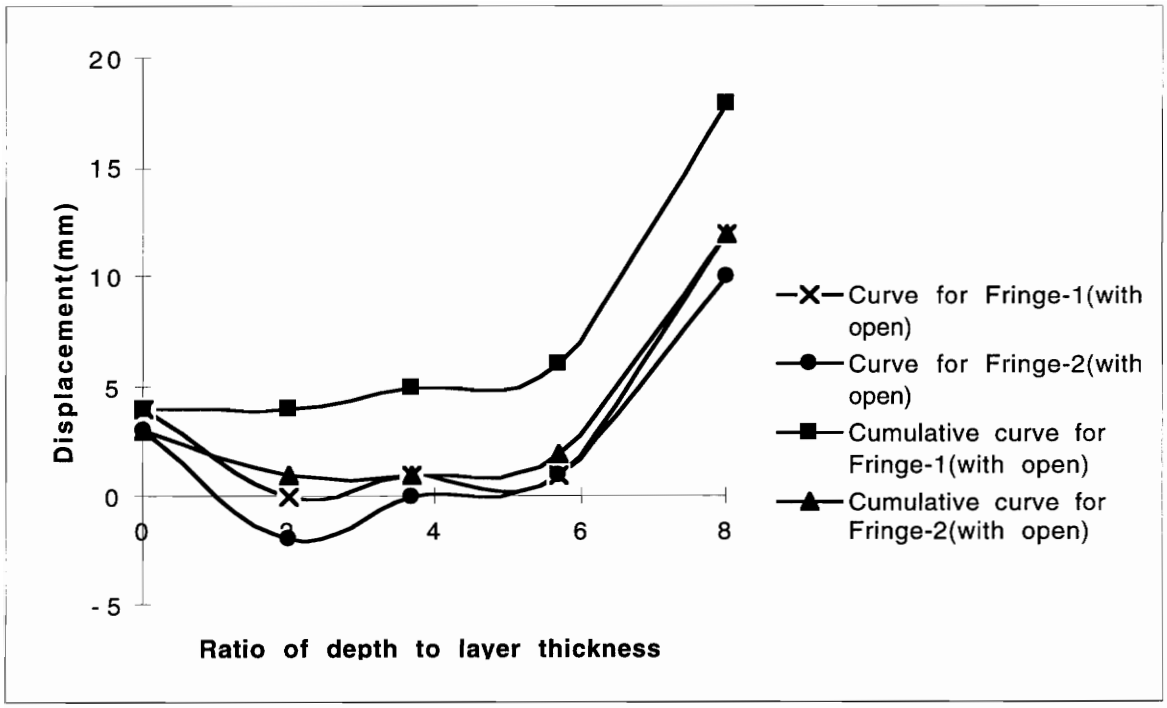

Figure 5.13 Effect of depth and thickness of layer on lateral spread of stress for 0.15 inch layer (with an opening)

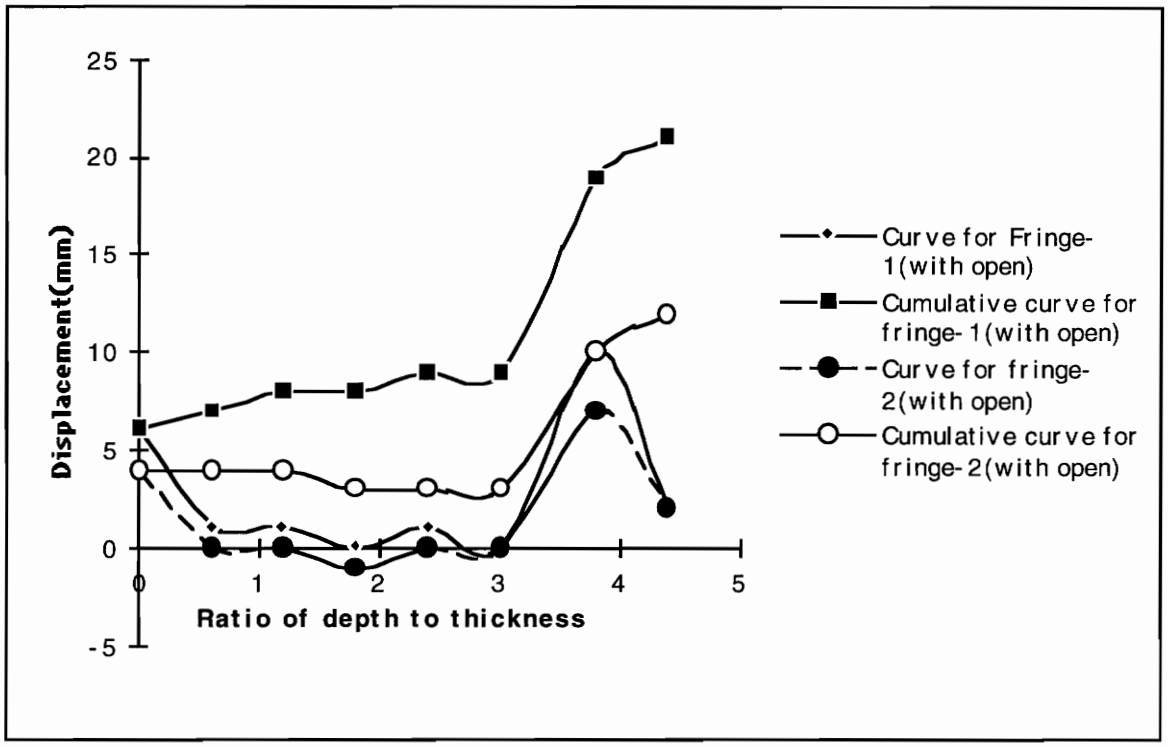

Figure 5.14 Effect of depth and thickness of layer in a 0.25 in layer with opening in the bottom layer.

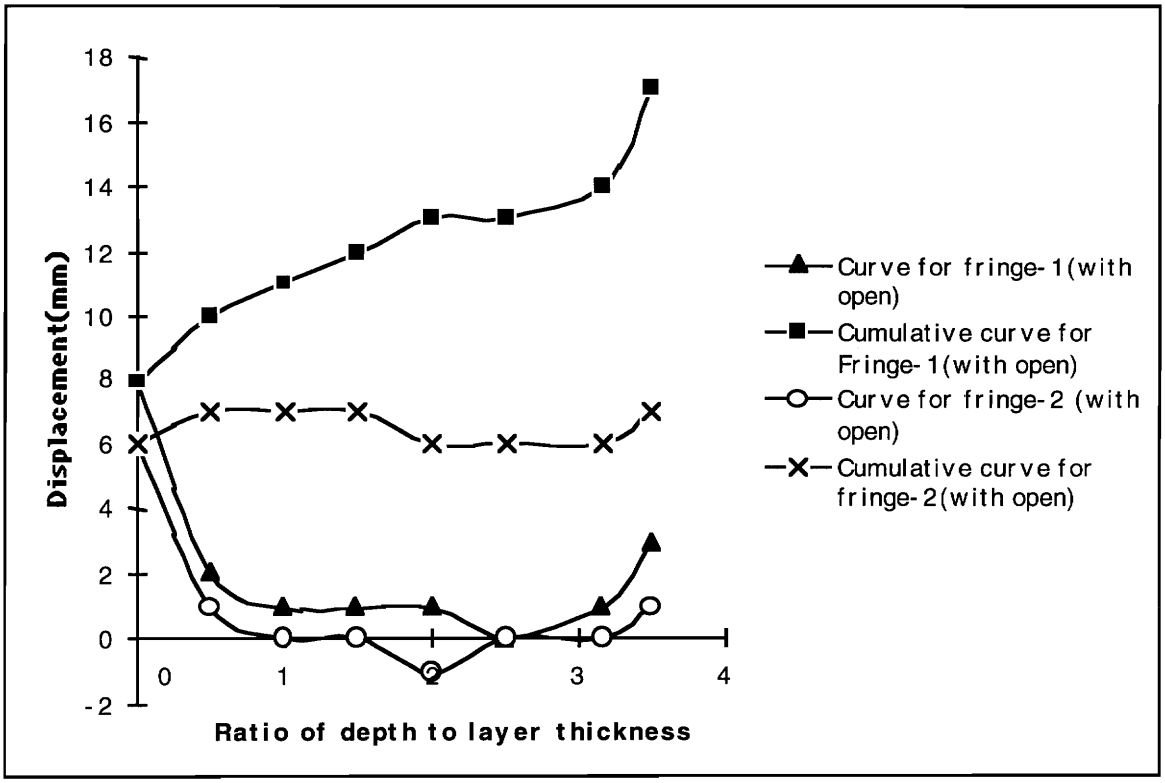

Figure 5.15 Effect of thickness and depth on 0.3 layer (with opening)

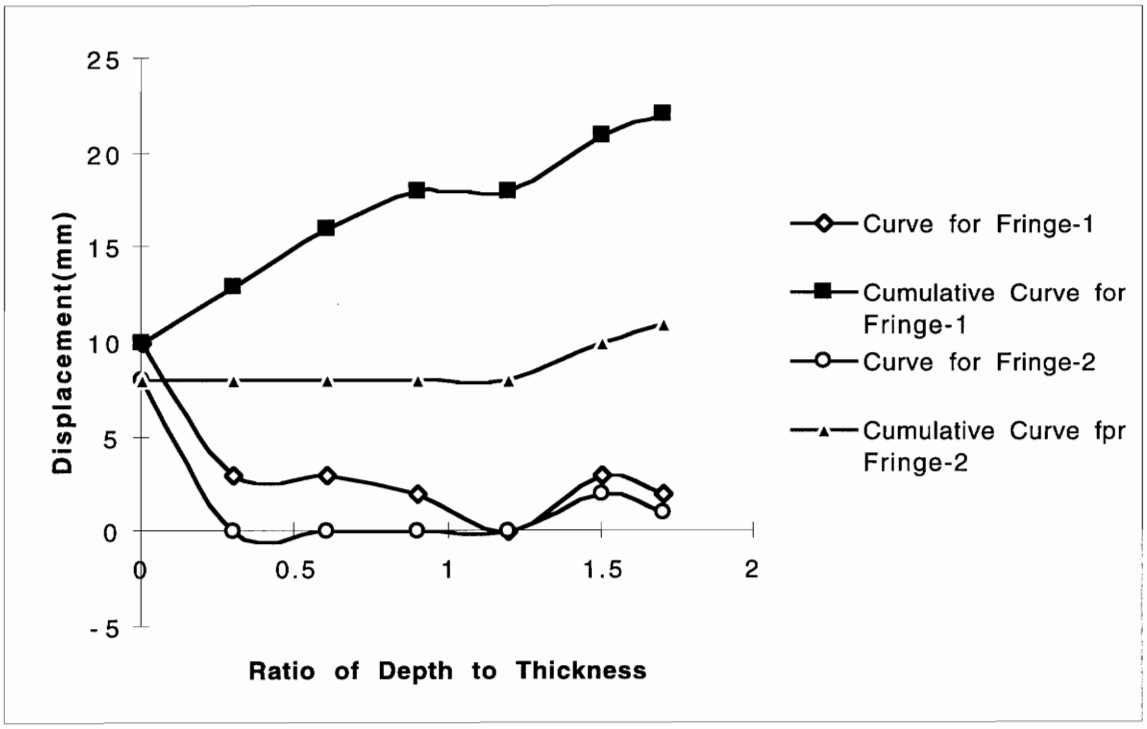

Figure 5.16 Effect of depth and thickness on lateral spread of stress layer in a 12.7 mm (0.5 inch) layer (with an opening in the bottom layer)

opening.

In conclusion, the following observations can be made regarding the effect of depth and thickness on the lateral spread of stress:

i) Thin layers tend to increase the lateral spread of stress up to a greater depth than thick layers. The stress bulb is hence elongated for thin layers.

ii) Lateral spread increases up to a depth of 1.5 times the thickness for thick layers and up to 8 times the thickness for thin layers.

iii) Openings tend to increase the lateral spread of stress.

5.2 Effect of the Number of Layers

The layering density or number of layers in the strata affects two aspects of stress transfer :

i) lateral spread of stress and

ii) magnitude of stress transferred to layers below.

Both these aspects were investigated. Figure 5.17 shows the variation of stress in the reference layer with different numbers of layers. Throughout the experiments, the total innerburden was kept constant at 1.5 inches, i.e., the reference layer was 1.5 inches below the load. The number of layers was varied from 1 to 9 and the stress and lateral spread of stress in the reference layer was studied.

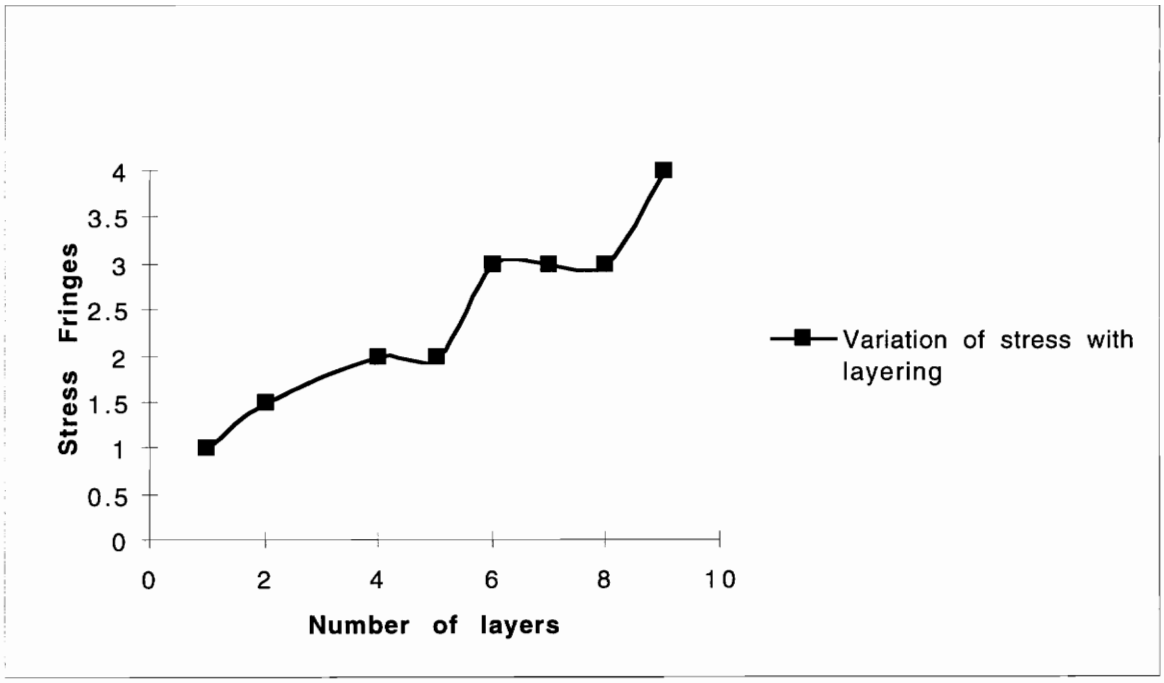

Figure 5.17 Variation of stress with layering

It can be seen from Figure 5.17 that as the number of layers increased, more stress was transferred. The variation in stress transfer was found to be linear with the number of layers. The phenomenon of stress increase with layering is best studied in combination with the variation in lateral spread of stress with layering. Figure 5.18 shows the variation of spread in the reference layer with layering. For a small increase in the number of layers, only an increase in the lateral spread occurs without any significant change in the stress. Additional layering increases the stress while decreasing the spread. This is evident in Figure 5.18. Stress increase occurs in places where there is a decrease in spread.

To summarize the effect of layering :

i) Layering increases stress transfer i.e., the more the number of layers, the more severe is the stress transfer.

ii) Layering causes lateral spread of stress, with thick layers increasing lateral spread more than thin layers.

iii) From Figure 5.17, it can be seen that *as the number of layers doubles, stress transfer also doubles*. Broadly, stress transfer and layering are linearly related.

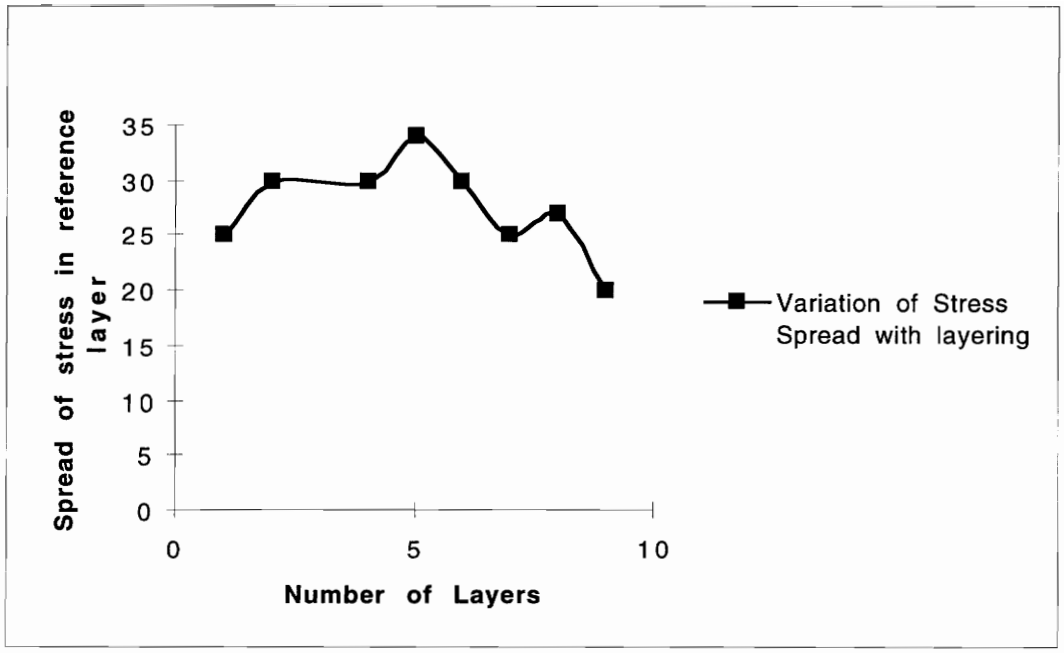

Figure 5.18 Variation in lateral spread of stress in reference layer with layering

5.3 Effect of Slippage between Layers

To study the effect of a low interlayer friction angle, a combination of grease and oil were introduced between the various layers. The experimental setup was the same as that shown in Figure 5.7. The effect of slippage on stress transfer also depends on the number of layers, since the greater the number of layers, the more the slippage. The effect of load on the slippage was also investigated. The experiments were a repeat of those described in Section 5.2. The difference was in the creation of a low friction angle between layers. Each set was tested at three different loads : 2.51 psi, 3.13 psi and 5.64 psi.

Figure 5.19 shows the effect of slippage with varying number of layers for 2.51 psi load. The pattern is similar to the those observed in the previous section for varying numbers of layers. It is clearly evident, however, that the stress transfer is greater for slip conditions. For 3.13 psi (Figure 5.20), results are similar to the high interlayer friction conditions, but for 5.64 psi (Figure 5.21), the stress transfer was increased significantly. From the above results it can be concluded that slippage between layers increases stress transfer, with the magnitude increasing significantly for larger loads (Figure 5.22).

Slippage also affects the lateral spread of stress. Figure 5.23 shows the effect of slippage on lateral spread of stress for a load of 2.51 psi. The feature immediately evident is that the spread is less for slip conditions. These findings were repeated for 3.13 psi and 5.64 psi loads (Figures 5.24 and 5.25). Thus, it can be concluded that slippage reduces lateral spread of stress (Figure 5.26).

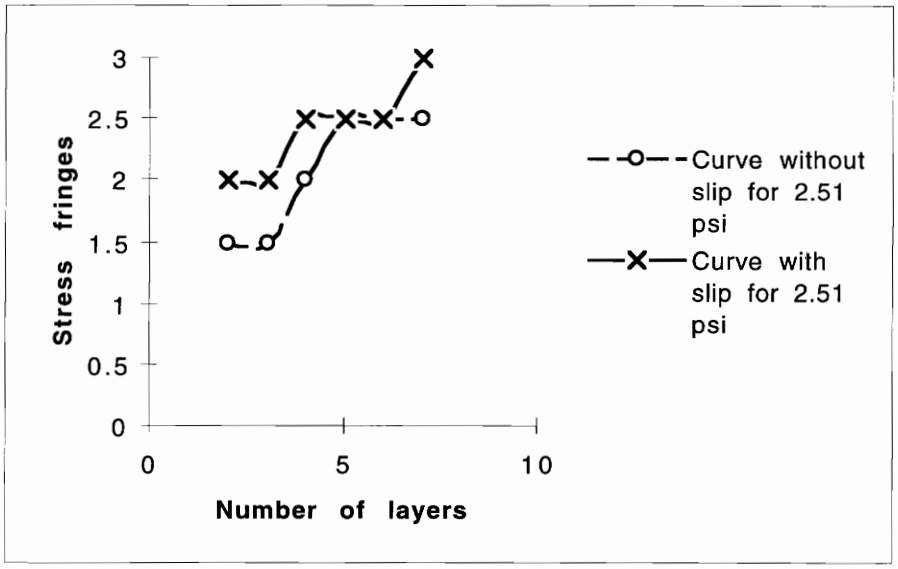

Figure 5.19 Stress for slip and no-slip conditions for 2.51 psi load

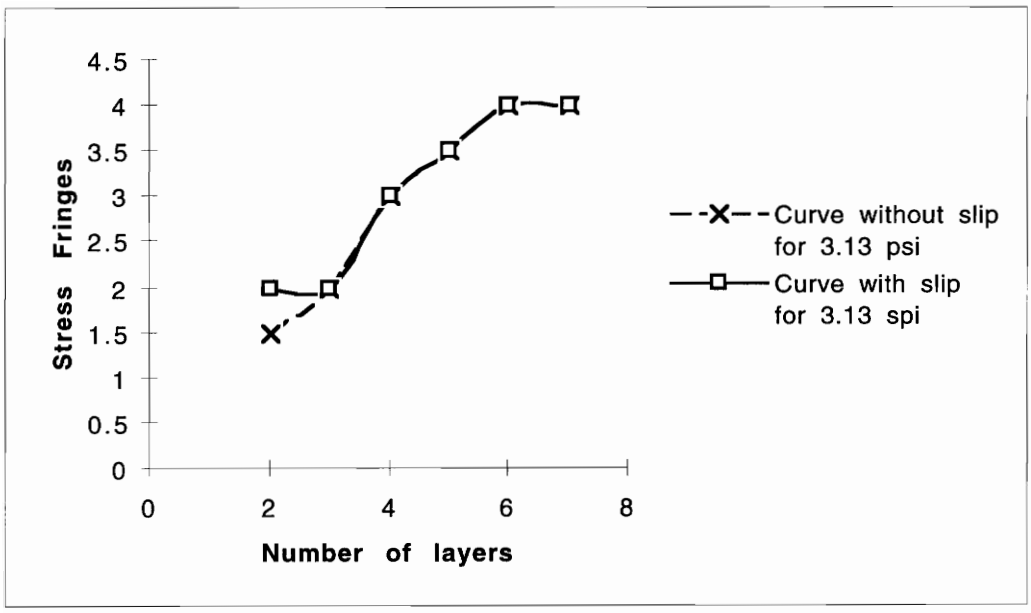

Figure 5.20 Stress for slip and no-slip conditions for 3.13 psi load

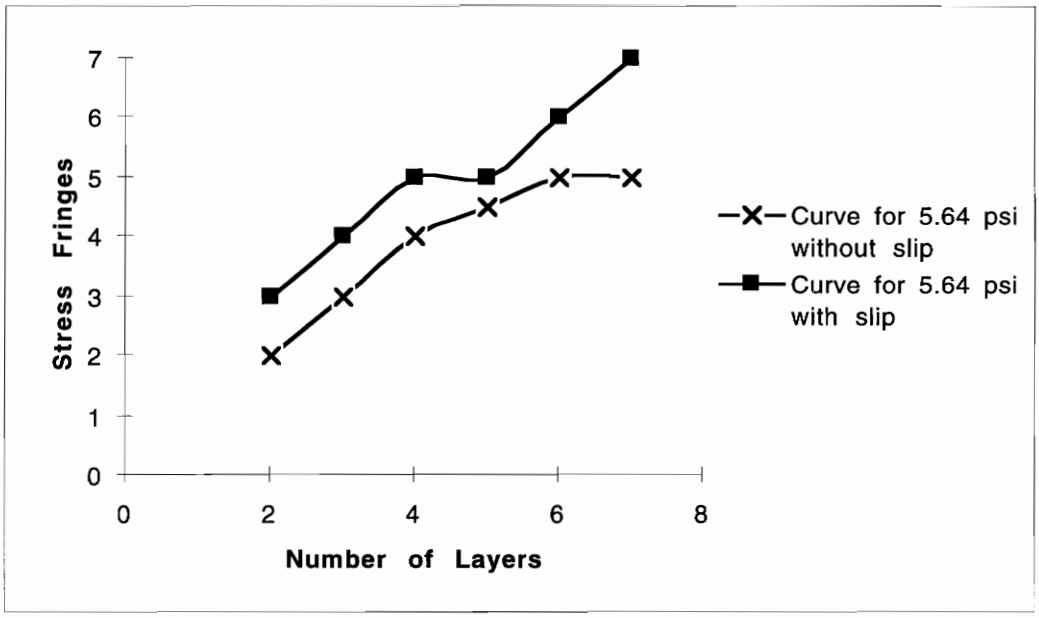

Figure 5.21 Stress for slip and no-slip conditions for 5.64 psi load

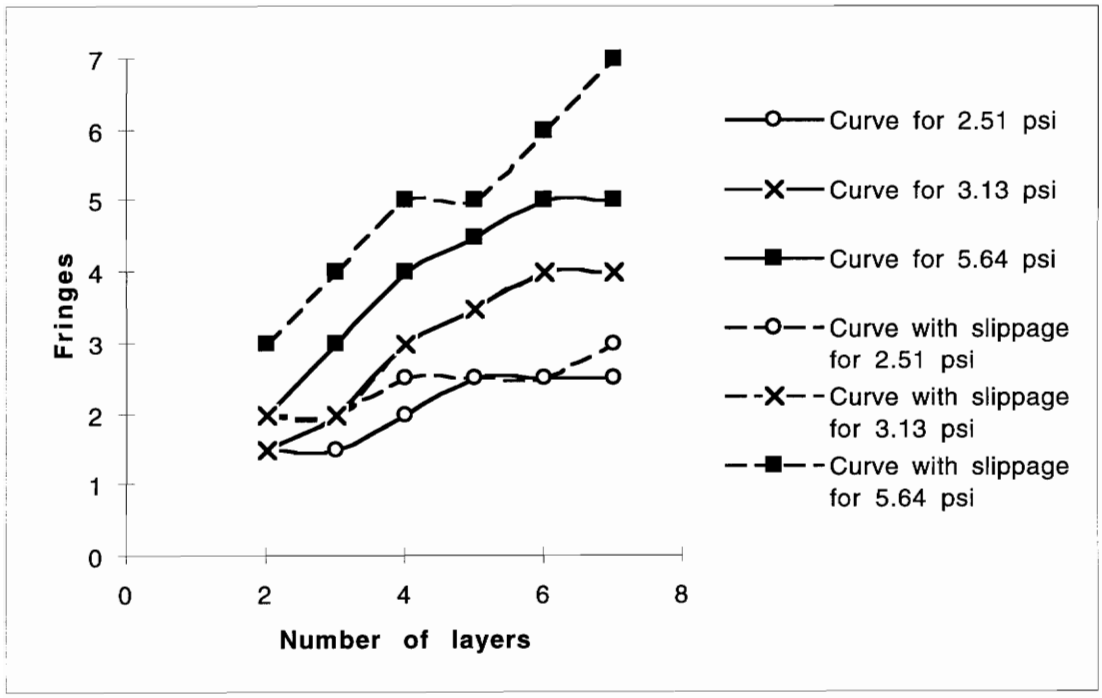

Figure 5.22 Effect of slippage on stress transfer with varying loads

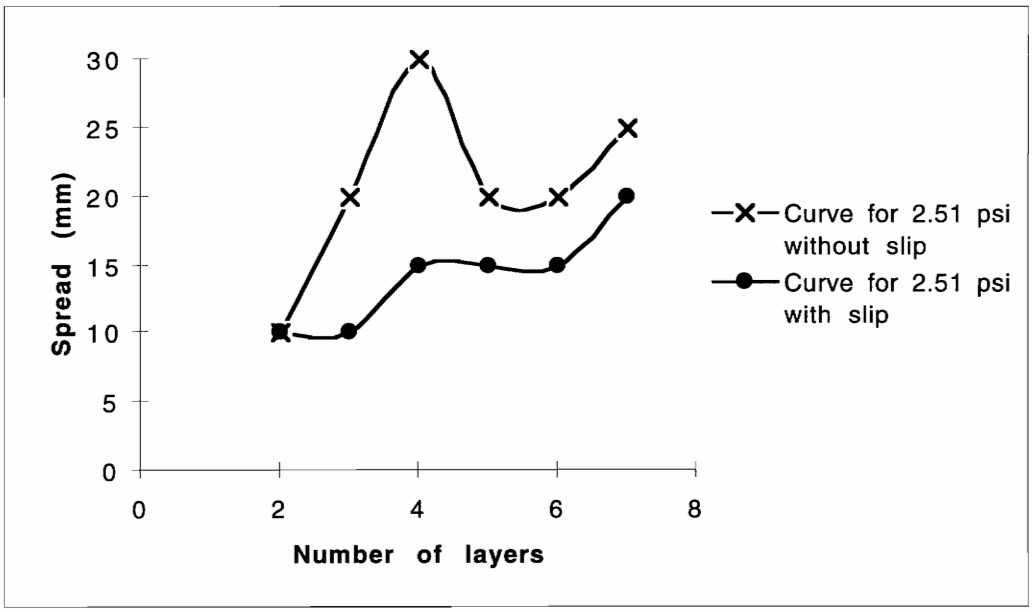

Figure 5.23 Lateral spread for slip and no-slip conditions for 2.51 psi load

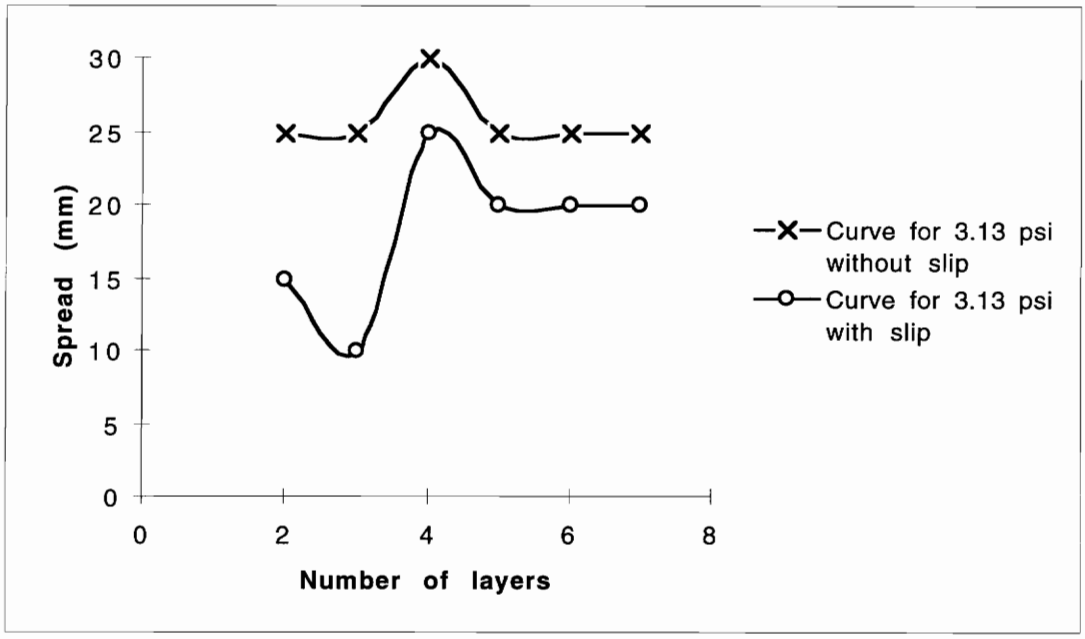

Figure 5.24 Lateral spread for slip and no-slip conditions for 3.13 psi load

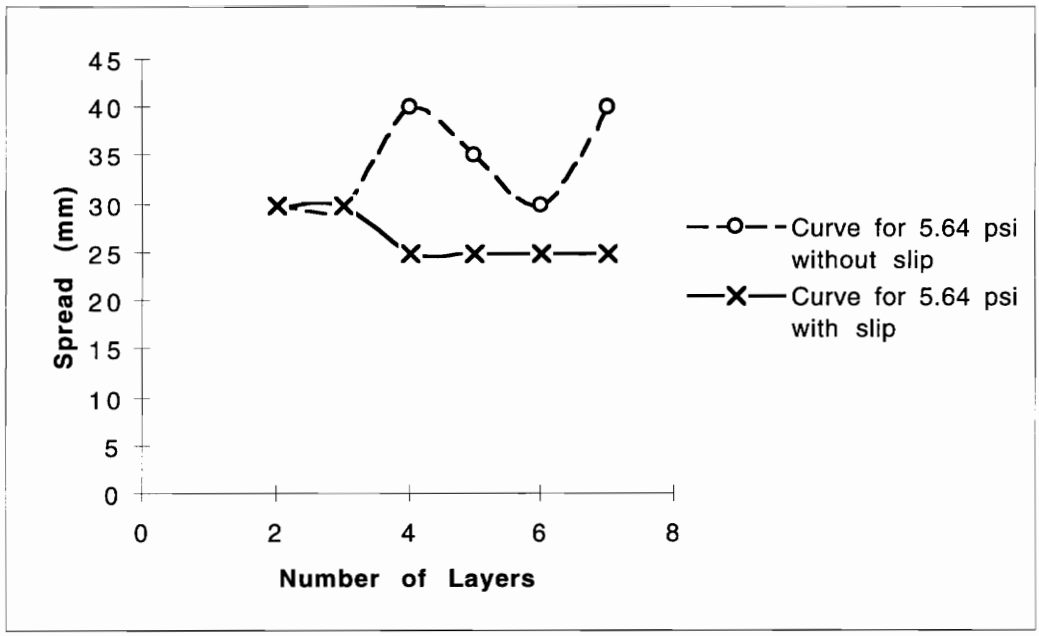

Figure 5.25 Lateral spread for slip and no-slip conditions for 5.64 psi load

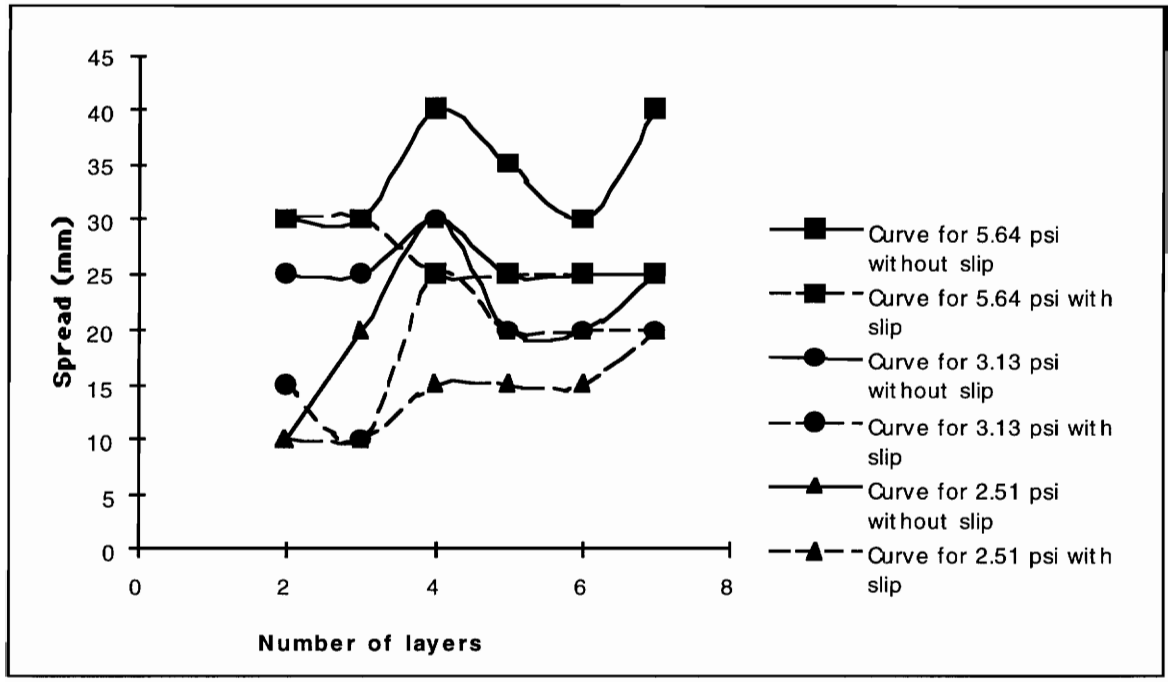

Figure 5.26 Effect of slippage on lateral spread of stress with varying loads

In conclusion, slippage affects stress transfer in the following ways :

i) It increases the magnitude of stress transfer with the effect being compounded by increased layering.

ii) It reduces the lateral spread of layering.

Chapter 6

CASE STUDIES

6.1 Laboratory Results and Prediction

Several mines were studied in an effort to develop a correlation between laboratory results and field observations. Data for the case studies were obtained from Stemple (1955).

Conclusions from laboratory studies were:

i) The stress above low modulus layers will be more severe than for high modulus layers.

ii) The stress below low modulus layers will be less than that for high modulus layers.

iii) Layers of high Young's Modulus transfer more stress than low modulus layers.

iv) Thick layers increase the lateral spread of stress.

v) Layering increases the severity of stress transfer, the layers, the more the stress transfer.

vi) Slippage between layers increases the magnitude of stress transfer and reduces the lateral spread.

6.2 Correlation with Field Observation

Case Study 1: The 36-70 inches thick Pocahontas No. 3 seam, located in McDowell County, West Virginia has the Pocahontas No. 4 seam 60-70 feet above it. Figure 6.1 shows the stratigraphy. The innerburden consists of layers of shales and some fairly thick sandstones. The Young's Modulus of the innerburden is thus high. The immediate roof and floor of the lower seam were good. Pocahontas No. 4, lying at a depth of 500 feet, was mined before the Pocahontas No.3. Bad roof conditions were experienced in Pocahontas No.3, *especially under the goaf-coal line* of the Pocahontas No.4 working. This confirmed the observations made in the laboratory that strata of high Young's Modulus transmitted stress more than low modulus strata.

Case Study 2: The Beckley seam, located in Raleigh County, West Virginia was mined earlier than the Pocahontas No.4, which was 285 feet below the Beckley seam (Figure 6.1). The overburden to the Beckley seam was 450 feet. The innerburden consisted of fairly firm strata of mostly shale with one 80 foot sandstone layer 50 feet above the lower seam. The rest of the innerburden was laminated. The Pocahontas No. 4 seam was 44 inches thick and was mined by longwall methods where the panels experienced stresses believed to be from the remnant structures left in the seam above, causing the failure of non-yielding type jacks and creating heavy roof falls. The immediate floor and roof were composed of strong strata. The extraction ratios were about the same for both the seams (80-85%). This behavior can only be explained by the fact that

Case Study : 1

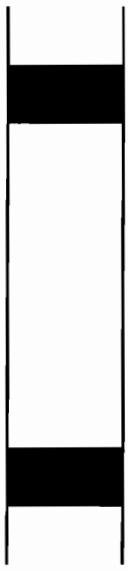

Depth : 500 ft

Pocahontas No.4 seam

Innerburden : 60-70 ft

Young's Modulus : High

Pocahontas No.3 seam

36-60 in. thick

Case Study :2

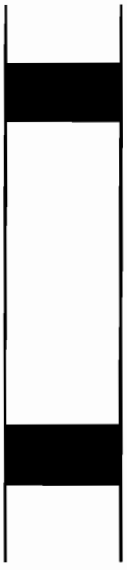

Depth : 450 ft

Beckley Seam

Innerburden : 285 ft

Young's Modulus : High

Pocahontas No.4 Seam

44 in. thick

Figure 6.1 Case Study 1 and 2

strong strata compounded with layering transferred more stress.

Case Study 3: The Upper Freeport seam, lying at an average depth of 150 feet below the surface, has the Lower Kittanning seam with an average thickness of 42 inches, 200 feet below it (Figure 6.2). The innerburden consisted of shales, unmined coal seams and other low modulus material. The roof and floor of the Lower Kittanning seam were medium hard and soft, respectively. The Upper Freeport seam was mined earlier than the Lower Kittanning seam. No disturbance was encountered in the lower seam due to upper seam workings. Soft and thick innerburden reduced the stress transfer from mining of the upper seam to the seam below. This conforms with the laboratory findings that low modulus layers transfer less stress.

Case Study 4: The following example compares and contrasts the effect of low modulus and hard innerburden on stress transfer (Figure 6.2). The Pocahontas No.4 and No.3 seams, located in McDowell County, West Virginia were mined simultaneously, as were the Sewickley and Pittsburgh seams, located in Magnolia County, West Virginia. The Pocahontas No. 4 seam was above the Pocahontas No. 3 seam while the Sewickley seam was above the Pittsburgh seam. The overburden to the upper seam in both cases was about 900 feet. The innerburden was about 90 feet between the seams. While the latter had low modulus innerburden, the former had sandstone innerburden. The workings in the Pocahontas No. 3 experienced weighting while the Pittsburgh seam did not. The extraction ratios in both the cases were about the same, for

Case Study :3

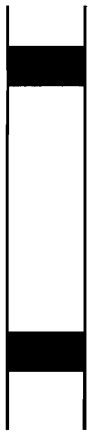

Depth :150 ft

Upper Freeport Seam

Innerburden : 200 ft (shale and other soft material)

Lower Kittaning seam
Thick : 42 in

Case Study: 4

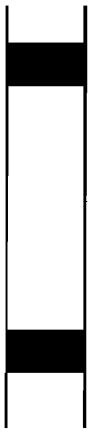

Depth :900 ft

Pocahontas No.4 Seam

Innerburden : 90ft
(high Young's Modulus)

Pocahontas No.3 Seam

McDowell Co, WV

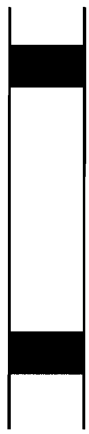

Depth :900ft

Sewickley seam

Innerburden :90 ft
(shale and other soft materia

Pittsburgh Seam

Magnolia Co., WV

Figure 6.2 Case Studies 3 and 4

both the upper and lower seams. The difference in stress transfer under almost similar conditions can be attributed to the difference in Young's Moduli of the innerburden with the softer innerburden transferring less stress.

Case Study 5: The Sewickley seam, lying at a depth of 1000 feet, has the Pittsburgh seam 65 feet below it (Figure 6.3). Both these seams are located in West Virginia. The extraction ratios in the lower and upper seams were 95% and 55%, respectively. There were two layers in the innerburden between the seams. The lower seam was found to be stable. In comparison, the Upper and Lower seams in Scotland had an innerburden of 71 feet where the Upper seam lay at a depth of 1160 feet (Ehgartner, 1982). The extraction rates in the two seams are unknown. The innerburden consisted of 13 layers and the conditions in the two cases were similar, save for the number of layers in the innerburden. While the former was stable, the latter was not. It can thus be reasoned that the increased number of layers in the second case increased the severity of the stress transfer leading to instability.

Case Study : 5

West Virginia, USA

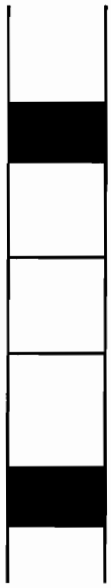

Depth : 1000 ft

Sewickley Seam
55% Extraction

Innerburden : 65 ft
(2 layers)

Pittsburgh Seam
95% Extraction

Scotland

Depth 1160 ft

Upper Seam

Innerburden : 71 ft
(13 layers)

Lower Seam

Figure 6.3 Case Study 5

Chapter 7

SUMMARY AND CONCLUSIONS

7.1 Summary

The results of the research can be summarized as follows:

Effect of Young's Modulus :

i) When layers of material vary in a given configuration, multiple layers of lower Young's Moduli transfer less stress than layers of high moduli or conversely, the stress *below* a low modulus layer is less than that below a high modulus layer.

ii) The stress *above* a lower modulus layer is greater than that for a higher modulus layer.

iii) The stress *above* a lower modulus layer can be up to two times the stress above a higher modulus layer, depending on the thickness of the layer and the Young's Moduli of the individual layers. This is true when the Young's Modulus of the higher modulus layer is up to a maximum of 10 times that of the lower modulus layer.

iv) The stress *below* a lower modulus layer is two to three times less than that for a layer with higher modulus, depending upon the thickness of the layer and the Young's Moduli of the layers.

However, for actual mining conditions or wherever the Young's Modulus for different strata material does not vary much, Young's modulus has little effect on stress transfer.

Effect of Layer Thickness :

i) Lateral spread of stress as seen in a pressure bulb increases with increasing thickness of the layer.

ii) The increase in lateral spread is almost linear until it maximizes, after which the spread decreases. This is because stress cannot be sustained over a large area through thick layers.

iii) Fringes of higher order stress have less spread than fringes of lower order stress, and an increase in load increases the spread.

iv) Thin layers tend to increase the lateral spread of stress to a *greater depth* than thick layers.

v) Lateral spread of stress increases up to a depth of 1.5 times the layer thickness for thick layers and 8 times the layer thickness for thin layers.

vi) Openings below the loading structures tend to increase the lateral spread of stress.

Effect of Number of Layers :

i) Layering increases stress transfer; that is, the greater the number of layers, the greater the stress transfer.

ii) Layering causes lateral spread of stress, where thicker layers increase lateral spread more than thinner layers.

iii) As the number of layers increases, the corresponding stress transfer also increases. Stress transfer and layering are linearly related.

Effect of Slippage on Stress Transfer between Layers :

i) Interlayer slippage increases the severity of stress transfer. The effect is greater for increased layering, i.e., more layers per unit thickness.

ii) Interlayer slippage reduces the lateral spread of stress.

Table 7.1 gives a concise summary of the research. Figure 7.1 gives a pictorial synopsis of the results.

7.2 Conclusions

Based on this research the following conclusions can be stated :

1) The geology and structure of the innerburden are the main factors that control stress transfer, both vertically and laterally.

2) A higher density of layering increases the vertical distance of stress transfer below highly stressed remnant structures in the upper seam when multiple seams occur in stratigraphic succession.

3) Layers of low modulus material transfer less stress than layers of high modulus material.

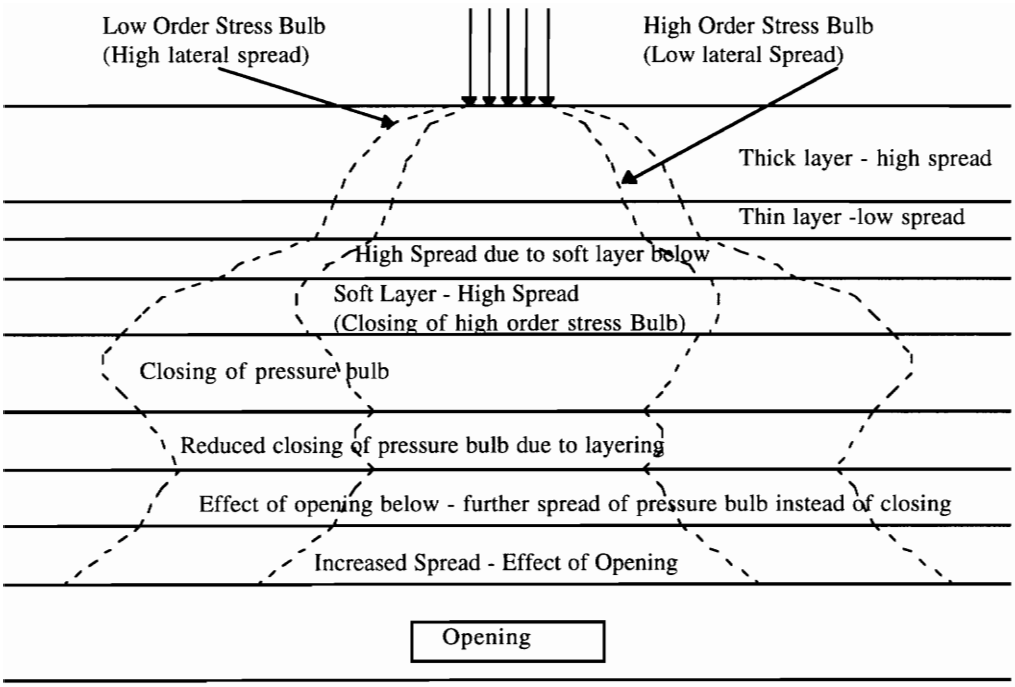

Figure 7.1 Pictorial synopsis of the research

Table 7.1. Summary of the research

Parameter	Results	Comments
Young's Modulus	Low Modulus layers (LML) transfer less stress below than high Modulus layers(HML)	Stress above LMLs high - upto 2 times that of HMLs Stress below HMLs high - upto 3 times that of HMLs Examples of LML@ : Bandera Shale, Y= 5.85 E+8 N/m^2 Examples of HML@ :Thorold Sandstone ,Y=6.9E+10 N/m^2; Fossiliferous Limestone, Y=7.08E+10 N/m^2
Layer Thickness	Lateral Spread increases with layer thickness	Thin layers increase pressure bulb width up to a greater depth than thick layers
Number of Layers	Layering increases stress transfer	Layering and stress transfer have a linear relationship
Coefficient of Friction	Low coefficient of friction increases stress transfer	The effect is compounded by layering

@ Carmichael, 1989.

4) Lateral spread of stress increases with increase in layer thickness.

5) Interlayer slip increases the magnitude of stress transfer through layered beds.

7.3 Recommendations

Future research in this field should include data collection, especially stress measurements, in active multi-seam mines. Most field validations of laboratory research are done indirectly which, while having the advantage of being inexpensive, may nevertheless not reflect the precise mechanism being studied. Hence, the understanding is never complete. The accurate quantification of the stress transfer mechanism required by the planners and designers in the coal mining industry can only be obtained by exhaustive field data collection. Whereas laboratory research helps in understanding the mechanisms, for quantification purposes it is preferred that data used for field correlations comes from the mine being studied.

The effect of large openings in the multiple seam mines should also be investigated. Most old workings have some sort of openings left behind, along with remnant structures, such as unmined pillars. This research has shown that these features affect stress transfer and serve to increase the lateral spread of stress. To have a realistic understanding of stress transfer in mutli-seam operations, large openings should also be investigated as to their effect on stress transfer.

Another problem which requires investigation is stress transfer in situations where there are more than two seams being worked. The stress transfer is complicated in these situations and needs to be better understood.

References

Akram, 1993, **Stability Assessment of Entry Roofs in Underlying Multiple Seams**, Ph.D Dissertation, Virginia Polytechnic Institute and State University, Blacksburg, June, p. 199.

Akram, M., Fraher, R., Haycocks, C. and Karmis, M., 1993, " Entry Design for Optimum Stability in a Multi-Seam Environment," **12th Conference on Ground Control in Mining**, Morgantown, WV.

Barko, E.N., 1982, **Mechanics of Interseam Failure in Multiple Horizon Mining**, M.S. Thesis, Virginia Polytechnic Institute and State University, Blacksburg, p. 195.

Beckett, L.A. and Madrid, R.S., 1988, **MULSIM / BM - A Structural Analysis Computer Program for Mine Design**, US Bureau of Mines Information Circular/1988, IC 9168, p.302.

Boussinesq, J., 1885, **Applicationes Potentiales a L`etude de l`equilibre et du Mouvement des Solides Elastiques**, Guathier-Villars, Paris.

Brady, B.H. and Brown, E.T., 1985, **Rock Mechanics for Underground Mining**, George Allen and Unwin Ltd., London, U.K.

Carmichael, R.S., 1989, **Practical Handbook of Physical Properties of Rocks and Minerals**, CRC Press, Boca Raton, FL, pp. 699-707.

Chekan, G.J., Matetic, R.J. and Galek, J.A., 1986, **Strata Interactions in Multiple-Seam Mining - Two Case Studies in Pennsylvania**, US Bureau of Mines Information Circular/1986, IC 9056, p.17.

Chekan, G.J. and Listak, J.M., 1992, **Analysis and Design Considerations for Superimposed Longwall Gate Roads**, US Bureau of Mines Information Circular/1994, IC 9305, p.14.

Chekan, G.J. and Listak, J.M., 1993, **Design Practices for Multi-Seam Longwall Mines**, Bureau of Mines Information Circular / 1993, IC 9360, p.35.

Chekan, G.J. and Listak, J.M., 1994, **Design Practices for Multi-Seam Room-and-Pillar Mines**, US Bureau of Mines Information Circular/1994, IC 9403, p.44.

Coates, D.F., 1965, **Pillar Loading**, Research Report, Dept. Of Mines and Technical Surveys, Ottawa, Canada.

Dally, J.W. and Riley, W.F., 1978, **Experimental Stress Analysis**, Second Edition, McGraw-Hill Book Company, p. 571.

Denkhaus, H.G., " Critical Review of Strata Movement Theories and Their Application to Practical Problems," **Journal of the South African Institute of Mining and Metallurgy**, Volume 64, pp. 310-332.

Desai, C.S. and Abel, J.F., 1972, **Introduction to Finite Element Method**, Von Nostrand Reinhold Co., New York.

Dinsdale, J.R., 1937, " Ground Failure Around Excavations," **Transactions of the Institution of Mining and Metallurgy**, London, Volume XLVI.

Dunham, R.K. and Stace, R.L., 1978, " Interaction Problems in Multi-seam Mining," Proceedings, **19th Symposium on Rock Mechanics**, Mackay School of Mines, Reno, NV, Vol. 1, pp.174-179.

Ehgartner, B.L., 1982, **Pillar Load Transfer Mechanisms in Multi-Seam Mining**, M.S Thesis, Virginia Polytechnic Institute and State University, Blacksburg, p.164.

Engineers International, Inc.,1981, **Investigation of Problems and Benefits of Underground Multiple Seam Coal Mining**," Final Technical Report, Department of Energy Contract DE-AC01- 70ET14242, p. 292.

Forrest, P., 1988, **Layout Design for Interactive Zones in Longwall Multiple Seam Mining**, M.S Thesis, Virginia Polytechnic Institute and State University, Blacksburg, p. 93.

Forrest, P. Haycocks, C. and Zhou, Y., 1988, "Design of Lower Seam Longwall Operations in Multiple Seam Mining," **7th Conference on Ground Control in Mining**, Morgantown, WV, pp. 43-50.

Fumagali, E., 1968, " Model Simulation of Rock Mechanics Problems," **Rock Mechanics in Engineering Practice**, John Wiley & Sons, London, pp. 353-384.

Gaziev, E. and Erilikhman, S., 1971, "Stress and Strain in Anisotropic Foundations," Proceedings, **Symposium on Rock Fractures**, ISRM, Paper II - 1, p. 10.

Giroud, J.P., 1970, " Stresses Under Linearly Leaded Rectangular Area," **Journal of The Soil Mechanics and Foundations Div.**, ASCE, Vol. 1, January.

Gerrard, C.M., 1967, "Stresses and Displacements in Layered Cross Anisotropic Elastic Systems," Proceedings, **New Zealand Conference on Soil Mechanics and Foundation Engineering**, August.

Haycocks, C. and Karmis, M., 1981, **Ground Control Mechanisms in Multi-Seam Mining**, **Performance Report** for the Office of Surface Mining, O.S.M Grant No. G5105050, July, 1981.

Haycocks, C. and Karmis, M., 1983, **Ground Control Mechanisms in Multi-Seam Mining,**", Final Report prepared for the Office of Mineral Institutes, Bureau of Mines, U.S. Department of the Interior, October, 1983.

Haycocks, C. and Zhou, Y., 1990, "Multiple-Seam Mining - A State-of-the-Art Review," Proceedings **9th Conference on Ground Control in Mining**, Morgantown, WV, pp. 1-11.

Haycocks, C., 1991, "Ground Control in Multi-Seam Mining," Proceedings, **22nd Annual Institute on Coal Mining Health, Safety and Research**, V.P.I & S.U Publication, Eds. E.Hugler., A. Bacho and M.Karmis, Blacksburg, p. 123-131.

Haycocks, C., Fraher, R., Haycocks,S.G. and Karmis, M., 1992, "Damage Prediction During Multi-Seam Mining," preprint, **Proc. SME-AIME**, Phoenix, Arizona.

Heuze, F.E., 1970, **The Design of Room and Pillar Structures in Competent Jointed Rock**, Doctor of Engineering Dissertation, University of California, Berkeley.

Holland, C.T., 1951, " Multiple Seam Mining," **Coal Age**, August, pp. 89-93.

Huang, Y.H., 1968, " Stresses and Displacements in Non-linear Soil Media," **Journal of the Soil Mechanics and Foundation Div**., ASCE, Vol. 2, January.

Hudock, S.D., 1983, **Effects of the Pressure Arch on Multiple Seam Mining**, M.S Thesis, Virginia Polytechnic Institute and State University, Blacksburg.

Iannachione, A.T., 1990, "The Effects of Roof and Floor Interface Slip on Coal Pillar Behavior," **Proc. 31st U.S. Symposium on Rock Mechanics**, Denver, CO, February, pp.153-160.

Kripakov, N.P., Sun, M.C. and Donato, D.A., 1994, " Automation of a Progressive Failure Procedure for Analysis of Underground Mine Pillar Designs," **Proc. 13th Conference on Ground Control in Mining**, Morgantown, WV, August, pp. 58-68.

Mark, C. and Bieniawski, Z.T., 1986, " An Empirical Method for the Design of Chain Pillars in Longwall Mining," Paper in Rock Mechanics: Key to Energy Production, **Proc. 29th U.S. Symposium on Rock Mechanics**, Tuscaloosa, AL, SME-AIME, pp. 415-422.

Mark, C., 1990, **Pillar Design for Longwall Mining**, US Bureau of Mines, IC 9247, p. 53.

Mark, C., 1991, " Practical Aspects of Longwall Pillar Design," **Proc. 10th Conference on Ground Control in Mining**, Morgantown, WV, August, pp. 1-13.

Mohr, F., 1956, "Influence of Mining on Strata," **Mine and Quarry Engineering**, Volume 22.

Mining Engineering, 1995, "Utility Demand will Fuel Record Coal Production in 1995," **Report** in **Mining Engineering**, March, p. 213.

National Coal Board, 1954, " Divisional Stress Control research Committee N.C.B., Durham and Northern Divisions Report of the Effects of Working in Adjacent Seams upon New Developments," **Transactions of the Institute of Mining Engineers**, Vol. 113, p.398.

Neall, G.M., 1975, **A Photoelastic Study of Roof Truss-Roof Interactions in Multilayered Mine Model**, M.S Thesis, Virginia Polytechnic Institute and State University, Blacksburg.

Obert, L. and Duvall, W.I., 1967, **Rock Mechanics and the Design of Structures in Rock**, John Wiley & Sons, Inc., New York, p. 645.

Pariseau, W.G., McDonald, M.M. Johnson, J.C. and Poad, M.E., 1992, "Personal Computer Finite Element Modeling for Ground Control and Mine Design," **Workshop**, **US Bureau of Mines**, Denver, CO, p. 43.

Peng, S.S., 1986., **Coal Mine Ground Control**, John Wiley & Sons, New York, p. 491.

Peng, S.S. and Chandra. U., 1980, "Getting the Most from Multiple Seam Reserves," **Coal Mining and Processing**, Vol. 17; pp. 78-84

Peng, S.S. and Chiang, H.S., 1984, **Longwall Mining**, Wiley, New York, p. 708.

Randolph, B.S., 1915, "The Theory of Arch in Mining," **The Colliery Engineer**, Volume 35, 1915, pp.427-429.

Rankilor, P.R. and McNicholas, J.B.,1968, "The Preparation and Use of a Stress Sensitive Material in Multi-layer Photoelastic Models," **Int. Journal. Rock Mech. & Min. Sci**., Vol. 5, pp. 465-476.

Scurfield, R.W., 1970, "Staffordshire Mining Layout for the mid-1970," **Mining Engineer**, Vol. 130, pp. 73-84.

Sowers, G.F., 1979, **Introductory Soil Mechanics and Foundations : Geotechnical Engineering**, 4th edition, Macmillan, New York.

Stemple, D.T., 1955, **A Study of Problems Encountered in Multiple-Seam Coal Mining in the Eastern United States**, M.S Thesis, Virginia Polytechnic Institute and State University, Blacksburg, p.125.

Su, W.H., Peng. S.S. and Hsuing, S.M., 1986, " Interactions in Multiple Seam Mining," Proceedings, **Engineering Health and Safety Symposium**, ed. A.W. Khair, SME-AIME, pp. 31-44.

Weisdack, G.V., 1995, "The Future of Longwall Mining Through 2005," **Coal Magazine**, February, pp. 45-47.

Whittaker, B.N. and Pye, J.H., 1975, "Design and Layout Aspects of Longwall Methods of Coal Mining," **Proc. 16th Sym. On Rock Mechanics,** pp. 303-328.

Wu, Wei, 1987, "**An Analysis of Close Seam Interaction Problems in the Appalachian Coal Fields**, Ph.D. Thesis, Virginia Polytechnic Institute and State University, Blacksburg.

Zhou, Y., 1988, **Designing for Upper Seam Stability**, Ph.D. Thesis, Virginia Polytechnic Institute and State University, Blacksburg.

Zhou, Y., 1989, " Evaluating the Impact of Mining an Underlying Seam on Recoverable Coal Reserves in an Overlying Seam," **28th International Geologic Congress**, Washington, D.C., July 9-19, pp 3-445, 3-446.

APPENDICES

A - I

THEORY OF PHOTOELASTICITY

Some transparent noncrystalline materials which are optically isotropic when free of stress become optically anisotropic and behave as crystals when they are exposed to increases in stress (Dally and Riley, 1978). This behavior remains in effect on the material as long as the material is stressed but disappears as soon as the stress is removed. The optical anisotropy and stress anisotropy are represented by their respective ellipsoids. Figure A-1 shows a stress ellipsoid and an index ellipsoid. *Temporary double refraction*, as this behavior is called, was first discovered by Sir David Brewster. Photoelastic studies are based on this phenomenon.

The stress optic law, first propounded by Maxwell, states that the changes in the indices of refraction are linearly proportional to the loads (Dally and Riley, 1978). For a linear elastic material, this means that the changes in the indices of refraction are linearly proportional to the stress and strain. The stress optic law can be represented by the following equations :

$$n_1 - n_0 = c_1 \sigma_1 + c_2 (\sigma_2 + \sigma_3) \qquad \text{-- -- -- -- -- (A-1)}$$

$$n_2 - n_0 = c_1 \sigma_2 + c_2 (\sigma_3 + \sigma_1) \qquad \text{-- -- -- -- -- (A-2)}$$

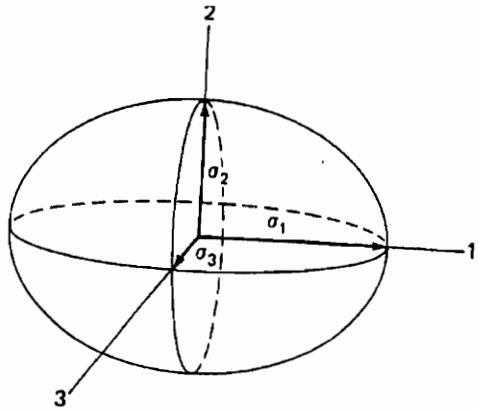

Stress Ellipsoid
(where s_1 ,s_2 ,s_3= principal stresses at a point)

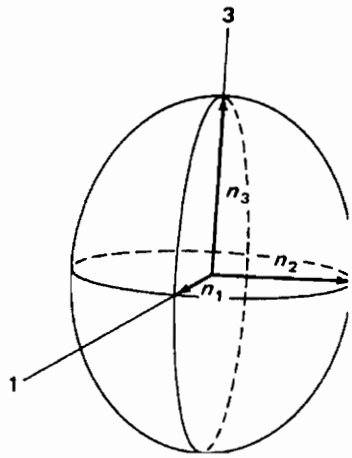

Index Ellipsoid

where n_1, n_2, n_3= indices of refraction of material in stressed state associated with principal stress directions (principal indices of refraction)

Figure A-1. The stress and index ellipsoids (After Dally and Riley, 1978)

$$n_3 - n_0 = c_1 \sigma_3 + c_2 (\sigma_1 + \sigma_2) \quad \text{-- -- -- -- --} \quad \text{(A-3)}$$

where $\sigma_1, \sigma_2, \sigma_3$ = principal stresses at a point

n_0 = index of refraction of material in unstressed state

n_1, n_2, n_3 = indices of refraction of material in stressed state associated with the principal stress directions (principal indices of refraction) and

c_1 and c_2 = constants known as stress-optic coefficients.

For plane stress conditions ($\sigma_3 = 0$) the equations reduce to

$$n_1 - n_0 = c_1 \sigma_1 + c_2 \sigma_2 \quad \text{-- -- -- --} \quad \text{(A-4)}$$

$$n_2 - n_0 = c_1 \sigma_2 + c_2 \sigma_1 \quad \text{-- -- -- --} \quad \text{(A-5)}$$

These absolute changes in index of refraction can be used to measure stress. In photoelastic methods, relative changes in index of refraction are measured rather than absolute changes. Further treatment of these equations given above shows that, for plane stress problems,

$$\Delta = \frac{2\Pi hc}{\lambda}(\sigma_1 - \sigma_2) \quad \text{-- -- -- -- --} \quad \text{(A-6)}$$

where

Δ = relative retardation

σ_1 and σ_2 = in-plane principal stresses, and σ_1 is greater than σ_2 but not greater than σ_0 if both in-plane stresses are compressive.

h = thickness of slice and

c = relative stress-optic coefficient

The relative stress-optic coefficient, *c,* is a material constant and is independent of the wavelength of the light being used. When the model material passes from the elastic to the plastic state, the relative stress-optic coefficient may depend on the wavelength of light used. This phenomenon is called *dispersion of birefringence* or *photoelastic dispersion.*

In this situation, equation (A-6) can be rewritten as :

$$\sigma_1 - \sigma_2 = \frac{Nf\sigma}{h} \quad N/m^2 \text{-- -- -- -- -- -- (A-7)}$$

where $N = \Delta / 2\pi$ (dimensionless)

is the relative retardation in terms of a complete cycle of retardation. Also

$f_\sigma = \lambda / c$ N / m

is the *material fringe value* of the model of thickness *h*. For practical purposes, equation (A-7) is sometimes written as

$$\Gamma_{max} = \frac{\sigma_1 - \sigma_2}{2} = \frac{Nf\sigma}{h} \text{-- -- -- -- -- -- (A-8)}$$

where Γ_{max} = maximum shear stress at a point in the photoelastic model and

f_σ = half of f_σ defined in equation (A-7).

APPENDIX II

Photograph of the Experimental Setup

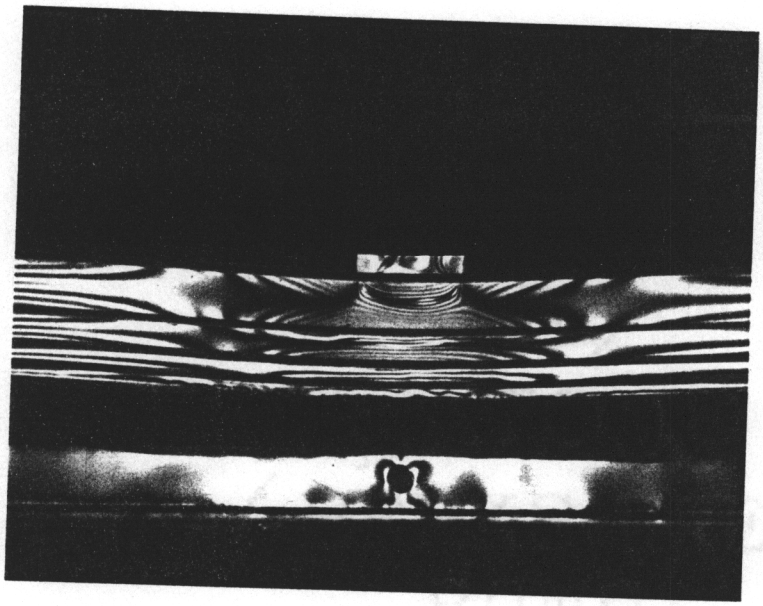

VITA

The author was born in West Bengal, India. He went to school in three different states in India. He graduated with distinction in Mining Engineering from Kothagudem School of Mines, Osmania University, India, in June 1991. He won the All India Mining Quiz in 1990 and the All India Student Technical Paper contest in 1991. After graduation he worked as a mining engineer for Hindustan Copper Limited at Malanjkhand Copper Project for more than two years. Awarded an assistantship, he enrolled in the Department of Mining and Minerals Engineering at Virginia Tech in Spring 1994 in the Master of Science program, where he is at present pursuing the Master's degree in Mining and Minerals Engineering.